

# Temperature-dependent gap equations and their solutions in the SU(4) model of high-temperature superconductivity

Yang Sun<sup>(1),\*</sup> Mike Guidry<sup>(2),†</sup> and Cheng-Li Wu<sup>(3)‡</sup>

<sup>(1)</sup>*Department of Physics, University of Notre Dame, Notre Dame, Indiana 46556, USA*

<sup>(2)</sup>*Department of Physics and Astronomy, University of Tennessee, Knoxville, Tennessee 37996, USA*

<sup>(3)</sup>*Physics Division, National Center for Theoretical Science, Hsinchu, Taiwan 300, ROC*

(Dated: November 19, 2018)

Temperature-dependent gap equations in the SU(4) model of high- $T_c$  superconductivity are derived and analytical solutions are obtained. Based on these solutions, a generic gap diagram describing the features of energy gaps as functions of doping  $P$  is presented and a phase diagram illustrating the phase structure as a function of temperature  $T$  and doping  $P$  is sketched. A special doping point  $P_q$  occurs naturally in the solutions that separates two phases at temperature  $T = 0$ : a pure superconducting phase on one side ( $P > P_q$ ) and a phase with superconductivity strongly suppressed by antiferromagnetism on the other ( $P < P_q$ ). We interpret  $P_q$  as a quantum phase transition point. Moreover, the pairing gap is found to have two solutions for  $P < P_q$ : a small gap that is associated with competition between superconductivity and antiferromagnetism and is responsible for the ground state superconductivity, and a large gap without antiferromagnetic suppression that corresponds to a collective excited state. A pseudogap appears in the solutions that terminates at  $P_q$  and originates from the competition between  $d$ -wave superconductivity and antiferromagnetism. Nevertheless, this conclusion does not contradict the preformed pair picture conceptually if the preformed pairs are generally defined as any pairs formed before pairing condensation.

PACS numbers: 71.10.-w, 74.20.Mn, 74.25.Dw, 74.72.-h

## I. INTRODUCTION

The properties of high-temperature (high- $T_c$ ) superconductivity in copper oxide materials pose a strong challenge to the theoretical understanding of superconductivity in strongly correlated many-body systems. The main question concerning the high- $T_c$  superconductivity phase diagram is the transition between the antiferromagnetic (AF) and superconducting (SC) phases, which is dominated by anomalous properties commonly attributed to a pseudogap in the spectrum [1]. Partly because of the complicated material properties and the nature of the experiments performed, different experiments seem to emphasize different aspects of the system, leading to different and sometimes contradictory possibilities for explanation of observables [2]. Many models have been proposed in the last two decades but there is no consensus as to the origin of the pseudogap properties. Still, one cannot answer the question: what is the real phase diagram in cuprates?

Describing collective motion in a strongly correlated many-body system in terms of single particle degrees of freedom is not always feasible. In the cuprate systems exhibiting high- $T_c$  superconducting properties, there is a substantial point of view (see, for example, Ref. [3]) that the many-body correlations are so strong that the dynamics can no longer be described meaningfully in terms of individual fundamental particles. However, collective

motions in such quantum many-body systems are often governed by only *a few* collective degrees of freedom. Once these degrees of freedom are identified and properly incorporated into a model, calculations may become feasible and, more importantly, the physics may become transparent. One systematic approach to this program of identifying the relevant collective degrees of freedom in a many-body system is the method of dynamical symmetries.

Examples of using the dynamical symmetry approach to study many-body problems may be found in nuclear physics [4, 5], molecular physics [6, 7], and particle physics [8]. Recently, we have developed an SU(4) dynamical symmetry model [9, 10, 11] aimed at understanding the mechanism that leads to high- $T_c$  superconductivity in cuprates. Theoretical models employing algebras and groups have been used in condensed matter physics (for recent examples, see Refs. [12, 13]). However, to our knowledge, the powerful dynamical symmetry methods that we employ here have not been applied systematically in this field.

In this paper we derive and solve the temperature-dependent gap equations in the SU(4) model. We demonstrate that this model can provide important insight into the puzzling issues associated with cuprate superconductors. In the next section we outline the SU(4) model (a more detailed description can be found in Refs. [9, 10, 11]). Temperature-dependent gap equations of the SU(4) model are derived in section III. Analytical solutions for the gap equations at  $T = 0$  are obtained in section IV, and a generic gap diagram (energy gaps versus doping at  $T = 0$ ) predicted by the SU(4) model is presented. The solutions of the gap equations at finite

---

\*Electronic address: ysun@nd.edu

†Electronic address: guidry@utk.edu

‡Electronic address: clwu@phys.cts.nthu.edu.tw

temperature are given in section V and these are used to construct a generic phase diagram in section VI. Finally, a summary is given in section VII. Technical details concerning construction, derivation, and solution of the gap equations are given in three appendixes.

## II. THE SU(4) MODEL

It is by now widely agreed that in cuprates, the mechanism responsible for superconductivity is closely related to the unusual antiferromagnetic insulator properties of their normal states. There are also compelling arguments that the pair mechanism leading to high- $T_c$  superconductivity does not correspond to ordinary BCS s-wave pairing. Phase-sensitive experiments indicate that the SC phase of most cuprates has  $d$ -wave-like pairing symmetry (at least for the hole-doped compounds), and this is also supported by photoemission experiments, which show the existence of nodal points in the quasiparticle gap.

Such observations argue strongly for a theory based on continuous symmetries of the dynamical system that is capable of describing more sophisticated pairing than found in the simple BCS picture, and capable of unifying SC and AF collective modes and the corresponding phases. Then such fundamentally different physics as SC order and AF order can emerge from the same effective Hamiltonian as global variables (e.g., doping and temperature) are varied.

### A. Basic ingredients of the SU(4) model

The basic assumption of the SU(4) model [9] is that the configuration space is built from *coherent pairs* formed from two electrons (or holes) centered on adjacent lattice sites. [The SU(4) model is particle-hole symmetric [14]. For cuprate superconductors one is generally interested in hole-doped compounds but more general applications of SU(4) can deal with either electrons or holes. Hereafter, unless specified explicitly, we use “electrons” to reference either electrons or holes.] In cuprates the coherent pairs are believed to exhibit  $d$ -wave orbital symmetry [15], and we assume a coexistence of two kinds of coherent pairs in a minimal model: the spin-singlet ( $D$ ) and the spin-triplet ( $\pi$ ) pairs. We adopt the  $d$ -wave pairs with structure defined in Refs. [13, 16] as the basic *dynamical building blocks* of the SU(4) model

$$\begin{aligned} D^\dagger &\equiv p_{12}^\dagger = \sum_k g(k) c_{k\uparrow}^\dagger c_{-k\downarrow}^\dagger & D &= (D^\dagger)^\dagger, \\ \pi_{ij}^\dagger &\equiv q_{ij}^\dagger = \sum_k g(k) c_{k+Q,i}^\dagger c_{-k,j}^\dagger & \pi_{ij} &= (\pi_{ij}^\dagger)^\dagger, \end{aligned} \quad (1)$$

where  $c_{k,i}^\dagger$  creates an electron of momentum  $k$  and spin projection  $i, j = 1$  or  $2$  ( $\equiv \uparrow$  or  $\downarrow$ ),

$$g(k) = (\cos k_x - \sin k_y)$$

is the  $d$ -wave form factor, and  $Q = (\pi, \pi, \pi)$  is an AF ordering vector. These pair operators, when supplemented with operators of particle-hole type  $\mathcal{Q}_{ij}$  and  $S_{ij}$ ,

$$\begin{aligned} \mathcal{Q}_{ij} &= \sum_k c_{k+Q,i}^\dagger c_{k,j} \\ S_{ij} &= \sum_k c_{k,i}^\dagger c_{k,j} - \frac{1}{2}\Omega\delta_{ij}, \end{aligned} \quad (2)$$

constitute a 16-element operator set that is closed under a  $U(4) \supset U(1) \times SU(4)$  algebra if the condition

$$g(k) \approx \text{sgn}(\cos k_x - \cos k_y)$$

is imposed. In Eq. (2),  $\Omega$  is the maximum number of doped electrons that can form coherent pairs, assuming the normal state (at half filling) to be the vacuum. The U(1) factor in  $U(1) \times SU(4)$  is associated with charge-density waves and is independent of the SU(4) algebra. The charge-density waves can be excluded in the symmetry limit and in the following discussion we shall restrict attention to the SU(4) subgroup. The 15 SU(4) generators are related to more physical operators through the linear combinations

$$\begin{aligned} \vec{S} &= \left( \frac{S_{12} + S_{21}}{2}, -i \frac{S_{12} - S_{21}}{2}, \frac{S_{11} - S_{22}}{2} \right) \\ \vec{Q} &= \left( \frac{\mathcal{Q}_{12} + \mathcal{Q}_{21}}{2}, -i \frac{\mathcal{Q}_{12} - \mathcal{Q}_{21}}{2}, \frac{\mathcal{Q}_{11} - \mathcal{Q}_{22}}{2} \right) \\ \vec{\pi}^\dagger &= \left( i \frac{q_{11}^\dagger - q_{22}^\dagger}{2}, \frac{q_{11}^\dagger + q_{22}^\dagger}{2}, -i \frac{q_{12}^\dagger + q_{21}^\dagger}{2} \right) \\ D^\dagger &= p_{12}^\dagger & D &= p_{12} \\ \hat{n} &= \sum_{k,i} c_{k,i}^\dagger c_{k,i} = S_{11} + S_{22} + \Omega \end{aligned} \quad (3)$$

where  $\vec{S}$  is the spin operator,  $\vec{Q}$  the staggered magnetization,  $\vec{\pi}^\dagger$  ( $\vec{\pi}$ ) the vector form of the creation (annihilation) operator of spin-triplet pairs, and  $\hat{n}$  the electron number operator. It will also sometimes prove useful to replace the number operator  $\hat{n}$  with the charge operator  $M$ , defined through

$$M = \frac{1}{2}(S_{11} + S_{22}) = \frac{1}{2}(\hat{n} - \Omega).$$

It has been demonstrated [11] that this SU(4) algebra defines the minimal symmetry implementing a unified description of antiferromagnetism and  $d$ -wave superconductivity that is consistent with Mott-insulator properties for normal states.

### B. The group structure and model Hamiltonian

The SU(4) group has three dynamical symmetry group chains:

$$\begin{aligned} &\supset SO(4) \times U(1) \supset SU(2)_s \times U(1) \\ SU(4) &\supset SO(5) \supset SU(2)_s \times U(1) \\ &\supset SU(2)_p \times SU(2)_s \supset SU(2)_s \times U(1) \end{aligned} \quad (4)$$

each of which ends in the subgroup  $SU(2)_s \times U(1)$  representing total spin and charge conservation. An  $SU(4)$  model Hamiltonian containing one and two-body interactions can then be determined uniquely,

$$H = \varepsilon \hat{n} + v \hat{n}^2 - G_0 D^\dagger D - G_1 \vec{\pi}^\dagger \cdot \vec{\pi} - \chi \vec{Q} \cdot \vec{Q} + \kappa \vec{S} \cdot \vec{S}. \quad (5)$$

In Eq. (5), the parameters  $G_0$ ,  $G_1$ , and  $\chi$  are effective interaction strengths of  $d$ -wave singlet pairing, triplet pairing, and staggered magnetization, respectively,  $\varepsilon$  is the average single-electron energy, and  $v$  may be interpreted as the mean value of the two-body interaction. In later discussions, we shall set  $\varepsilon = v = 0$  because the first two terms in Eq. (5) are state-independent and provide only a constant energy. The term  $\kappa \vec{S} \cdot \vec{S}$  will also be ignored for the present discussion, corresponding to assuming the total spin for the ground state to be zero.

Using the properties of Lie algebras, we have shown [9] that analytical solutions for matrix elements can be obtained for the group chains defined in (4). Each symmetry limit has been shown to represent a *collective mode* that corresponds to properties observed in the cuprate phase diagram: the  $SO(4)$  limit is associated with an AF phase occurring when  $\chi$  is dominant ( $G_0 = G_1 < \chi$ ), the  $SU(2)_p$  limit is associated with a  $d$ -wave SC phase occurring when  $G_0$  is dominant ( $\chi = G_1 < G_0$ ), and the  $SO(5)$  limit is a critical dynamical symmetry [10] representing a transitional phase that is soft against AF and pairing fluctuations (occurring when  $G_0 = \chi$ ). A more extensive discussion of these symmetry limits and their corresponding phases can be found in Refs. [9, 10].

### C. Doping dependence in the $SU(4)$ model

The phenomenology of the cuprate superconductors suggests that the expectation value of the system Hamiltonian should depend microscopically on the amount of hole doping. Within the  $SU(4)$  model it is doping that drives the system from one dynamical symmetry limit to another, causing the system to undergo crossovers and phase transitions. Let us now explore this microscopic doping dependence of the  $SU(4)$  model in more detail.

The lowest-order Casimir operators  $C_g$  for each subgroup  $g$  in (4) are

$$\begin{aligned} C_{SO(4)} &= \vec{Q} \cdot \vec{Q} + \vec{S} \cdot \vec{S} \\ C_{SO(5)} &= \vec{\pi}^\dagger \cdot \vec{\pi} + \vec{S} \cdot \vec{S} + M(M-3) \\ C_{SU(2)_p} &= D^\dagger \cdot D + M(M-1) \\ C_{SU(2)_s} &= \vec{S} \cdot \vec{S} \\ C_{U(1)} &= M \text{ and } M^2. \end{aligned}$$

The  $SU(4)$  quadratic Casimir operator is

$$C_{SU(4)} = D^\dagger \cdot D + \vec{\pi}^\dagger \cdot \vec{\pi} + \vec{Q} \cdot \vec{Q} + \vec{S} \cdot \vec{S} + M(M-4), \quad (6)$$

which is an invariant in the  $SU(4)$  representation space.

In the general case we may introduce a seniority-like quantum number  $n_b = u\Omega$ , which is the number of particles in the system that do not couple to  $D$  or  $\pi$  pairs, with  $u$  being the number density of the unpaired particles. For the  $u = 0$  case, we take as a Hilbert space

$$\begin{aligned} |u=0\rangle &= |n_x n_y n_z n_d\rangle \\ &= (\pi_x^\dagger)^{n_x} (\pi_y^\dagger)^{n_y} (\pi_z^\dagger)^{n_z} (D^\dagger)^{n_d} |0\rangle, \end{aligned}$$

which is a collective subspace (the  $D$ - $\pi$  pair space) associated with  $SO(6)$  irreps of the form  $(\sigma_1, \sigma_2, \sigma_3) = (\frac{\Omega}{2}, 0, 0)$ . [Because  $SO(6)$  and  $SU(4)$  have the same Lie algebra we choose to label  $SU(4)$  irreps with  $SO(6)$  quantum numbers.] The expectation value of the  $SU(4)$  Casimir operator (6) for  $u = 0$  is

$$\langle C_{SU(4)} \rangle = \frac{\Omega}{2} \left( \frac{\Omega}{2} + 4 \right),$$

and is a constant for any state in the  $D$ - $\pi$  pair space. More generally, states with  $n_b$  unpaired particles can be described by irreps of the form  $(\frac{1}{2}(\Omega - n_b), 0, 0)$ . Thus for the  $u \neq 0$  case with broken pairs the expectation value of the  $SU(4)$  Casimir operator is

$$\langle u | C_{SU(4)} | u \rangle = \frac{\Omega}{2} \left( \frac{\Omega}{2} + 4 \right) - \frac{n_b}{2} \left( \Omega - \frac{n_b}{2} + 4 \right).$$

For a system with charge  $\langle M \rangle = \frac{1}{2}(n - \Omega)$ , the  $SU(4)$  invariance leads to a conserved quantity

$$\begin{aligned} \mathcal{E}_{SU4} &= D^\dagger D + \vec{\pi}^\dagger \cdot \vec{\pi} + \vec{Q} \cdot \vec{Q} + \vec{S} \cdot \vec{S} \\ &= C_{SU4} - M(M-4). \end{aligned}$$

The expectation value  $\langle \mathcal{E}_{SU4} \rangle$  is thus a constant, independent of how the system changes its state within the  $SU(4)$  space. It follows that in the large  $\Omega$  limit,

$$\langle \mathcal{E}_{SU4} \rangle = \frac{\Omega^2}{4} [(1-u)^2 - x^2] \quad x = 1 - \frac{n}{\Omega}, \quad (7)$$

where  $n$  is the electron number. In the above expressions,  $x$  may be regarded as the relative doping fraction in our theory. Since  $\Omega - n$  is the hole number when  $n < \Omega$ , positive  $x$  represents the case of hole-doping, with  $x = 0$  corresponding to half filling (no doping) and  $x = 1$  to maximal hole-doping. Negative  $x$  ( $n > \Omega$ ) is defined naturally as the relative doping fraction for electron-doping.

The true doping rate, defined as  $P = (\Omega - n)/\Omega_e$ , where  $\Omega_e$  is the number of lattice sites, is related to  $x$  through

$$P = x \frac{\Omega}{\Omega_e} = x P_f, \quad P_f \equiv \frac{\Omega}{\Omega_e},$$

with  $P > 0$  for hole doping and  $P < 0$  for electron doping.  $P_f$  can be regarded as the maximum possible value of the true doping rate  $P$ . Experimentally,  $P_f$  is found to be  $0.23 \sim 0.27$  [1].

### D. No-double-occupancy and maximum doping

The SU(4) group is the minimal symmetry accommodating superconductivity and antiferromagnetism in cuprates. It is further found that the SU(4) symmetry is a consequence of non-double-occupancy – the constraint that each lattice site cannot have more than one valence electron. It has been demonstrated [11] that with no approximation to the  $d$ -wave formfactor  $g(k)$ , the momentum-space operator sets (1) and (2) may be expressed in the coordinate space as

$$\begin{aligned}
p_{12}^\dagger &= \sum_{r=\text{even}} \left( c_{\mathbf{r}\uparrow}^\dagger c_{\mathbf{r}\downarrow}^\dagger - c_{\mathbf{r}\downarrow}^\dagger c_{\mathbf{r}\uparrow}^\dagger \right) \\
q_{ij}^\dagger &= \sum_{r=\text{even}} \left( c_{\mathbf{r},i}^\dagger c_{\mathbf{r},j}^\dagger + c_{\mathbf{r},j}^\dagger c_{\mathbf{r},i}^\dagger \right) \\
S_{ij} &= \sum_{r=\text{even}} \left( c_{\mathbf{r},i}^\dagger c_{\mathbf{r},j} - c_{\mathbf{r},j}^\dagger c_{\mathbf{r},i}^\dagger \right) \\
\tilde{Q}_{ij} &= \sum_{r=\text{even}} \left( c_{\mathbf{r},i}^\dagger c_{\mathbf{r},j} + c_{\mathbf{r},j}^\dagger c_{\mathbf{r},i}^\dagger \right) \\
p_{12} &= (p_{12}^\dagger)^\dagger \quad q_{ij} = (q_{ij}^\dagger)^\dagger.
\end{aligned} \tag{8}$$

In Eq. (8), the summation is over even sites of the lattice, the quantity  $\tilde{Q}_{ij}$  is defined by

$$\tilde{Q}_{ij} \equiv Q_{ij} + \frac{1}{2} \delta_{ij} \Omega,$$

and  $c_{\mathbf{r},i}^\dagger$  ( $c_{\mathbf{r},i}$ ) creates (annihilates) an electron of spin  $i$  located at  $\mathbf{r}$ , while  $c_{\mathbf{r}\pm\mathbf{a},i}^\dagger$  ( $c_{\mathbf{r}\pm\mathbf{a},i}$ ) creates (annihilates) an electron of spin  $i$  at its four neighboring sites,  $\mathbf{r} \pm \mathbf{a}$  and  $\mathbf{r} \pm \mathbf{b}$ , with equal probabilities ( $\mathbf{a}$  and  $\mathbf{b}$  are the crystal constants along the  $\mathbf{x}$  and  $\mathbf{y}$  directions, respectively, on the copper-oxide plane),

$$c_{\mathbf{r}\pm\mathbf{a},i}^\dagger = \frac{1}{2} \left( c_{\mathbf{r}+\mathbf{a},i}^\dagger + c_{\mathbf{r}-\mathbf{a},i}^\dagger - c_{\mathbf{r}+\mathbf{b},i}^\dagger - c_{\mathbf{r}-\mathbf{b},i}^\dagger \right).$$

Explicit commutation operations show that only if the no-double-occupancy constraint is imposed, so that the anticommutator relation

$$\left\{ c_{\mathbf{r},i}^\dagger, c_{\mathbf{r}',i'}^\dagger \right\} = \delta_{\mathbf{r}\mathbf{r}'} \delta_{ii'}$$

is valid, does the operator set (8) close under the  $U(1) \times \text{SU}(4)$  Lie algebra. Thus, the coordinate-space commutation algebra of the operators (8) demonstrates that SU(4) symmetry *necessarily implies* a no-double-occupancy constraint in the copper oxide conducting plane. This suggests a fundamental relationship between SU(4) symmetry and Mott-insulator normal states at half filling for cuprate superconductors.

One immediate conclusion [11] is that the no-double-occupancy constraint sets an upper limit for the number of doped holes if SU(4) is to be preserved exactly:  $\Omega_{\text{max}} = \frac{1}{4} \Omega_e$ . Thus, the maximum doping fraction consistent with SU(4) symmetry is

$$P_{\text{f}} \equiv \frac{\Omega}{\Omega_e} = \frac{1}{4}.$$

Beyond this doping fraction the no-double-occupancy condition cannot be ensured and exact SU(4) symmetry cannot be preserved. The empirical maximum doping fraction  $0.23 \sim 0.27$  for cuprate superconductivity may then be taken as indirect evidence for a strongly-realized SU(4) symmetry underlying the superconductivity in cuprates.

### III. GAP EQUATIONS IN THE SU(4) MODEL

Equation (4) defines three dynamical symmetry group chains, each representing a collective mode. Analytical solutions associated with these symmetry limits have been derived [9]. However, a realistic physical system may not lie in any of these dynamical symmetry limits. In order to study properties of a realistic system and phase transitions between the symmetry limits, one needs systematic ways to deal with approximate symmetries. There is a well-developed theoretical approach to relating a many-body algebraic theory to an approximation of that theory that exhibits spontaneous symmetry breaking: the method of generalized coherent states [10, 17]. This method is a variational procedure using the coherent state as the trial wavefunction in a quasiparticle space. It may be viewed as the most general Hartree–Fock–Bogoliubov variational formulation, but with an additional proviso that the variational states are constrained to respect the highest symmetry of a set of group chains, as in Eq. (4). Generalized coherent states are thus particularly suitable for studying the ground state properties of any strongly correlated many-body system that is amenable to a dynamical symmetry description.

#### A. The generalized coherent-state method

The coherent state  $|\psi\rangle$  associated with the SU(4) symmetry can be written formally as

$$|\psi\rangle = \mathcal{T} |0^*\rangle, \tag{9}$$

with the operator  $\mathcal{T}$  defined by

$$\mathcal{T} = \exp(\eta_{00} p_{12}^\dagger + \eta_{10} q_{12}^\dagger - \text{h. c.}). \tag{10}$$

In Eq. (9),  $|0^*\rangle$  is the physical vacuum (the ground state of the system), the real parameters  $\eta_{00}$  and  $\eta_{10}$  are symmetry-constrained variational parameters, and h. c. stands for the Hermitian conjugate. Since the variational parameters weight the elementary excitation operators  $p_{12}^\dagger$  and  $q_{12}^\dagger$  in Eq. (10), they represent collective state parameters for a  $D$ - $\pi$  pair subspace truncated under the SU(4) symmetry [18].

The symmetry-constrained variational Hamiltonian is

$$H' = H - \lambda \hat{n},$$

where  $H$  is the Hamiltonian (5) and  $\lambda$  is the chemical potential, determined by requiring particle-number conservation. The parameters  $\eta_{00}$  and  $\eta_{10}$  in Eq. (10) are determined by the variational principle  $\delta\langle H' \rangle = 0$ , where  $\langle H' \rangle$  is the expectation value of  $H'$  with respect to the ground state  $|0^*\rangle$

$$\langle H' \rangle \equiv \langle 0^* | H' | 0^* \rangle.$$

As shown in Appendix A, it is convenient to evaluate the variation  $\delta\langle H' \rangle = 0$  using a 4-dimensional matrix representation that was introduced in Refs. [10, 19]. In this representation the unitary operator  $\mathcal{T}$  implements a transformation from the original particle basis to a quasiparticle basis and the variation parameters  $\eta_{00}$  and  $\eta_{10}$  are replaced, respectively, by  $u_{\pm}$  and  $v_{\pm}$ , with a unitary condition  $u_{\pm}^2 + v_{\pm}^2 = 1$ . Under this transformation the basic fermion operators

$$\{c_{\mathbf{r}\uparrow}^{\dagger}, c_{\mathbf{r}\downarrow}^{\dagger}, c_{\mathbf{r}\uparrow}, c_{\mathbf{r}\downarrow}\}$$

are converted to quasiparticle operators

$$\{a_{\mathbf{r}\uparrow}^{\dagger}, a_{\mathbf{r}\downarrow}^{\dagger}, a_{\mathbf{r}\uparrow}, a_{\mathbf{r}\downarrow}\},$$

as shown explicitly in Eq. (A4). This implies that

$$\begin{aligned} (u_+ c_{\mathbf{r}\uparrow} + v_+ c_{\mathbf{r}\downarrow}^{\dagger}) |0^*\rangle &= a_{\mathbf{r}\uparrow} |\psi\rangle \\ (u_- c_{\mathbf{r}\downarrow} - v_- c_{\mathbf{r}\uparrow}^{\dagger}) |0^*\rangle &= a_{\mathbf{r}\downarrow} |\psi\rangle \\ (u_- c_{\mathbf{r}\uparrow}^{\dagger} + v_- c_{\mathbf{r}\downarrow}) |0^*\rangle &= a_{\mathbf{r}\uparrow}^{\dagger} |\psi\rangle \\ (u_+ c_{\mathbf{r}\downarrow}^{\dagger} - v_+ c_{\mathbf{r}\uparrow}) |0^*\rangle &= a_{\mathbf{r}\downarrow}^{\dagger} |\psi\rangle \end{aligned}$$

and one sees that this is a Bogoliubov-type transformation: each quasiparticle state is a mixture of a particle and a hole, and the coherent state  $|\psi\rangle$  is an SU(4)-symmetry constrained quasiparticle vacuum.

By using the matrix representation one can calculate expectation value for any operator  $\hat{O}$  in the coherent state representation through the transformation

$$\langle 0^* | \hat{O} | 0^* \rangle = \langle \psi | \mathcal{T} \hat{O} \mathcal{T}^{-1} | \psi \rangle.$$

Detailed derivations are given in Appendix A.

## B. Temperature dependence

At finite temperature,  $|\psi\rangle$  may no longer be a quasiparticle vacuum state and the quasiparticle annihilation operators acting on  $|\psi\rangle$  do not necessarily give zero. In Appendix B a formalism is derived to deal with the finite-temperature case. To formulate the simplest initial model we assume that at a temperature  $T$  the single-particle levels  $\varepsilon_{r\pm}$  (defined in Eq. (17) below) are degenerate and contain  $\tilde{n}_{r+} + \tilde{n}_{r-}$  quasiparticles. The quasiparticle number densities are then assumed to be given

by the Fermi-Dirac distribution

$$\tilde{n}_{\pm}(T) = \frac{2}{\Omega} \sum_{r=\text{even}} \tilde{n}_{r\pm}(T) = \frac{2}{1 + \exp(R e_{\pm}/k_B T)}, \quad (11)$$

where  $e_{\pm}$  is the quasiparticle energy defined in Eq. (16) below. In Eq. (11), we have introduced an energy scaling factor  $0 < R < 1$ . This is because the actual single-particle energies are generally non-degenerate so that the realistic quasiparticle excitation should be easier. Thus  $\tilde{n}_{\pm}(T)$  should in general be larger than those with the degenerate approximation. The factor  $R$  accounts for this effect in an average manner, and it may be determined by fitting to data.

For one-body operators at finite temperatures the expectation values are (see Appendix B)

$$\begin{aligned} \langle D^{\dagger} \rangle &= \langle D \rangle = -\frac{\Omega}{2} [P_+(T)u_+v_+ + P_-(T)u_-v_-] \\ \langle \pi_z^{\dagger} \rangle &= \langle \pi_z \rangle = -\frac{\Omega}{2} [P_+(T)u_+v_+ - P_-(T)u_-v_-] \\ \langle Q_z \rangle &= \frac{\Omega}{2} [P_+(T)v_+^2 - P_-(T)v_-^2] \\ \langle \hat{n} \rangle &= \frac{\Omega}{2} [P_+(T)(2v_+^2 - 1) + P_-(T)(2v_-^2 - 1) + 2] \\ \langle \pi_x \rangle &= \langle \pi_y \rangle = \langle \vec{S} \rangle = \langle Q_x \rangle = \langle Q_y \rangle = 0, \end{aligned} \quad (12)$$

where we have defined

$$P_{\pm}(T) = 1 - \tilde{n}_{\pm}(T) = \tanh\left(\frac{R e_{\pm}}{2k_B T}\right).$$

For the scalar products of these one-body operators the expectation values are products of the corresponding one-body ones in the large- $\Omega$  approximation,

$$\begin{aligned} \langle D^{\dagger} D \rangle &= \langle D \rangle^2 \\ \langle \vec{\pi}^{\dagger} \cdot \vec{\pi} \rangle &= \langle \pi_z \rangle^2 \\ \langle \vec{Q} \cdot \vec{Q} \rangle &= \langle Q_z \rangle^2 \\ \langle \vec{S} \cdot \vec{S} \rangle &= 0. \end{aligned} \quad (13)$$

If  $T \rightarrow 0$ , then  $P_{\pm}(T) \rightarrow 1$  and Eqs. (12) and (13) reduce to Eqs. (A9) and (A10), respectively.

## C. Energy gaps and gap equations

We now use the preceding results to express the variational Hamiltonian  $\langle H' \rangle$  in the coherent state representation. Introducing the energy gaps

$$\begin{aligned} \Delta_d &\equiv G_0 \sqrt{\langle D^{\dagger} D \rangle} \\ \Delta_{\pi} &\equiv G_1 \sqrt{\langle \vec{\pi}^{\dagger} \cdot \vec{\pi} \rangle} \\ \Delta_q &\equiv \chi \sqrt{\langle \vec{Q} \cdot \vec{Q} \rangle}, \end{aligned} \quad (14)$$

one obtains

$$\langle H' \rangle = (\varepsilon - \lambda)n - \left( \frac{\Delta_d^2}{G_0} + \frac{\Delta_{\pi}^2}{G_1} + \frac{\Delta_q^2}{\chi} \right).$$

Variation of  $\langle H' \rangle$  with respect to  $u_{\pm}$  or  $v_{\pm}$  (that is, solving  $\delta\langle H' \rangle = 0$ ) yields

$$2u_{\pm}v_{\pm}(\varepsilon_{\pm} - \lambda) - \Delta_{\pm}(u_{\pm}^2 - v_{\pm}^2) = 0,$$

which is satisfied by

$$\begin{aligned} u_{\pm}^2 &= \frac{1}{2} \left( 1 + \frac{\varepsilon_{\pm} - \lambda}{e_{\pm}} \right) \\ v_{\pm}^2 &= \frac{1}{2} \left( 1 - \frac{\varepsilon_{\pm} - \lambda}{e_{\pm}} \right), \end{aligned} \quad (15)$$

where

$$e_{\pm} = \sqrt{(\varepsilon_{\pm} - \lambda)^2 + \Delta_{\pm}^2} \quad (16)$$

and

$$\Delta_{\pm} = \Delta_d \pm \Delta_{\pi} \quad \varepsilon_{\pm} = \varepsilon \mp \Delta_q. \quad (17)$$

Inserting Eq. (15) into Eqs. (12 – 13) and employing the gap definitions (14), one obtains the temperature-dependent gap equations

$$\Delta_d = \frac{G_0\Omega}{4} (w_+ \Delta_+ + w_- \Delta_-) \quad (18a)$$

$$\Delta_{\pi} = \frac{G_1\Omega}{4} (w_+ \Delta_+ - w_- \Delta_-) \quad (18b)$$

$$\frac{4\Delta_q}{\chi\Omega} = w_+(\Delta_q + \lambda') + w_-(\Delta_q - \lambda') \quad (18c)$$

$$-2x = w_+(\Delta_q + \lambda') - w_-(\Delta_q - \lambda'), \quad (18d)$$

where we define

$$w_{\pm} \equiv \frac{P_{\pm}(T)}{e_{\pm}}, \quad (19)$$

and

$$\lambda' \equiv \lambda - \varepsilon. \quad (20)$$

By solving the above algebraic equations, all the gaps and the chemical potential  $\lambda'$  can be obtained. The total energy can be calculated as

$$\begin{aligned} E &= \langle H' \rangle + \lambda n \\ &= \varepsilon n - \left( \frac{\Delta_d^2}{G_0} + \frac{\Delta_{\pi}^2}{G_1} + \frac{\Delta_q^2}{\chi} \right). \end{aligned}$$

To simplify the discussion, we shall hereafter ignore the single-particle energy in the above equation by setting  $\varepsilon = 0$ , since this term has been approximated as a state-independent constant in our model and thus plays no role in the phase competition. We can then express the energy density  $E/\Omega$  as

$$\frac{E}{\Omega} = - \left( \frac{\Delta_d^2}{G_0\Omega} + \frac{\Delta_{\pi}^2}{G_1\Omega} + \frac{\Delta_q^2}{\chi\Omega} \right). \quad (21)$$

The three gaps  $\Delta_d$ ,  $\Delta_{\pi}$  and  $\Delta_q$  in the above equations represent, respectively, the characteristic energy scales of spin-singlet pairing, triplet pairing, and the AF correlation. Hence the ground state energy is determined by the three energy gaps. Once the gaps and the chemical potential  $\lambda'$  are known, the quasiparticle energies  $e_{\pm}$ , as well as the amplitudes  $u_{\pm}$  and  $v_{\pm}$ , can all be determined through Eqs. (15 – 17), permitting other ground state properties to be calculated.

These results are formally analogous to those of the BCS theory with  $v_{\pm}^2$  the probability of single particle levels  $\varepsilon_{\pm}$  being occupied,  $\Delta_{\pm}$  the energy gaps, and  $e_{\pm}$  the quasiparticle energies. The essential difference from BCS theory is that conventional pairing theories deal with one pairing gap and one kind of quasiparticle; here we have two kinds of quasiparticles and several energy gaps, implying a large variety of new physics.

In the formalism describing this more sophisticated pairing the quantities  $e_{\pm}$  are energies for two kinds of quasiparticle excitation, corresponding to two sets of non-degenerate single particle energy spectra  $\{\varepsilon_{\pm}\}$  separated by an energy  $2\Delta_q$ . Each level can be occupied by only one electron of either up or down spin. The corresponding pairing gaps are  $\Delta_{\pm}$ , which are linear combinations of the two gaps  $\Delta_d$  and  $\Delta_{\pi}$ . The probabilities for single-particle levels to be occupied or unoccupied are  $v_{\pm}^2$  and  $u_{\pm}^2$ , respectively.

In the following sections we shall give analytical solutions for the gap equations (18), first for zero temperature and then for finite temperatures. As we shall see, a rich phase structure emerges naturally in these solutions as a consequence of competition between the various energy scales.

#### IV. SOLUTION OF GAP EQUATIONS AND THE GAP DIAGRAM AT T = 0

There are three parameters,  $\chi$ ,  $G_0$ , and  $G_1$ , in the coupled algebraic equations (18), corresponding to the three elementary interactions in the SU(4) model: the AF correlation ( $\chi$ ), the spin-singlet pairing ( $G_0$ ), and the spin-triplet pairing ( $G_1$ ). Physical solutions of the gap equations depend on the choices for these parameters. Experimental evidence suggests that these three interactions in cuprates are all attractive, and we will demonstrate later that the AF correlation should be the strongest and the spin-triplet pairing the weakest. Thus, in the results presented below we assume

$$\chi > G_0 > G_1 > 0. \quad (22)$$

Analytical solutions for the gap equations assuming this condition can be obtained as follows.

### A. Solution of the gap equations at $T=0$

The gap solutions at  $T = 0$  can be written explicitly for two doping regimes separated by a special doping point given by

$$x_q = \sqrt{\frac{\chi - G_0}{\chi - G_1}}. \quad (23)$$

We shall interpret  $x_q$  as a *critical doping* marking a quantum phase transition because the wavefunctions and physical properties of the two doping regions lying on either side of this point at zero temperature are qualitatively different. Specifically, one finds the following solutions. (The general derivations of the gap solutions are given in Appendix C.)

(1) The all-gap solution for  $x \leq x_q$ :

$$\Delta_q = \frac{\chi\Omega}{2} \sqrt{(x_q^{-1} - x)(x_q - x)} \quad (24a)$$

$$\Delta_d = \frac{G_0\Omega}{2} \sqrt{x(x_q^{-1} - x)} \quad (24b)$$

$$\Delta_\pi = \frac{G_1\Omega}{2} \sqrt{x(x_q - x)} \quad (24c)$$

$$\lambda' = -\frac{\chi\Omega}{2} x_q(1 - x_q x) - \frac{G_1\Omega}{2} x. \quad (24d)$$

This is the most important solution that has all gaps non-zero and exists only for the doping range  $x \leq x_q$ . In addition, there are trivial solutions in which at least two gaps are zero.

(2) The pure spin-singlet pairing solution with  $\Delta_q = \Delta_\pi = 0$  is valid for the entire physical doping range  $0 \leq x \leq 1$  and given by

$$\Delta_q = \Delta_\pi = 0 \quad (25a)$$

$$\Delta_0 \equiv \Delta_d = \frac{G_0\Omega}{2} \sqrt{1 - x^2} \quad (25b)$$

$$\lambda' = -\frac{G_0\Omega}{2} x. \quad (25c)$$

This is also an important solution in that it gives the ground-state for  $x > x_q$  (see discussions below). It can be verified easily that both solutions (24) and (25) satisfy the SU(4) condition (7) with  $u = 0$ , which means that all electrons are paired at  $T = 0$ .

For completeness, we list below additional trivial solutions. These are a spin-triplet pairing solution, a pure AF solution, and a metal solution (with all gaps zero), all of which are valid for the entire physical doping range  $0 \leq x \leq 1$ :

(3) The spin-triplet pairing solution:

$$\Delta_q = \Delta_d = 0 \quad (26a)$$

$$\Delta_\pi = \frac{G_1\Omega}{2} \sqrt{1 - x^2} \quad (26b)$$

$$\lambda' = -\frac{G_1\Omega}{2} x. \quad (26c)$$

(4) The pure AF solution:

$$\Delta_d = \Delta_\pi = 0 \quad (27a)$$

$$\Delta_q = \frac{\chi\Omega}{2}(1 - x) \quad (27b)$$

$$\lambda' = -\frac{\chi\Omega}{2}(1 - x). \quad (27c)$$

(5) The metal solution:

$$\Delta_q = \Delta_d = \Delta_\pi = 0, \quad (28a)$$

$$\lambda' = -2kT \operatorname{atanh}(x) \quad (28b)$$

$$= 0 \text{ at } T = 0.$$

The trivial solutions can be verified easily. For example, when  $\Delta_q = 0$  one obtains immediately  $w_+ = w_-$  from Eq. (18c). There are two solutions satisfying Eqs. (18a) and (18b): either  $\Delta_d \neq 0$  and  $\Delta_\pi = 0$ , or  $\Delta_\pi \neq 0$  and  $\Delta_d = 0$ . The former gives the singlet pairing solution (25a – 25b) while the latter leads to the triplet pairing solution (26a – 26b). Eqs. (25c) and (26c) for  $\lambda'$  result from Eq. (18d). The AF solution is obtained because  $\Delta_d = \Delta_\pi = 0$  is a trivial solution of Eqs. (18a – 18b). The metallic state solution with all gaps vanishing is obvious from inspection of the equations.

We shall demonstrate below that these solutions contain rather rich physics as a function of doping. Among the five sets of gap solutions (Eqs. (24 – 28)), the one with the lowest energy at each doping corresponds to the physical ground state. We can calculate these energies by inserting the gap solutions directly into Eq. (21), and then investigate how these different sets of solutions compete with each other at  $T = 0$ . From Fig. 1, one sees clearly that the energy of the all-gap solution  $E_{\text{mix}}$  is always the lowest one and thus is the physical ground state for the doping range  $x \leq x_q$ . For  $x > x_q$ , the pure singlet pairing state becomes the ground state because  $E_d$  is the lowest energy for this doping range. All the other trivial solutions lie higher in energy. They may be regarded as collective excited states but they cannot become the physical ground state at  $T = 0$ .

As we will see later in the study of phase transitions, for  $T > 0$  the AF or the metallic state could become the ground state in certain temperature and doping ranges. However, note that this can never happen for the spin-triplet pairing state, as long as  $G_1$  is the weakest of the three coupling parameters. In other words, although spin-triplet pairing plays an important role in the SU(4) theory, the pure spin-triplet state can never be reached by thermal excitations as long as the condition (22) is satisfied.

### B. Gap diagram at $T=0$

A generic gap diagram at  $T = 0$  describing features of the energy gaps as functions of doping  $x$  is shown in Fig. 2. The diagram is constructed using the analytical

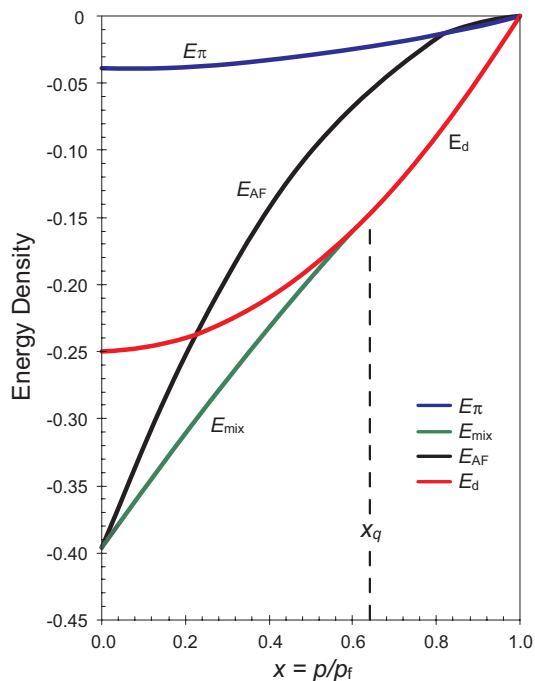


FIG. 1: (Color online) Total energy associated with different gap solutions at  $T = 0$ .  $E_{\text{mix}}$  is the energy calculated with the all-gap solution (24), while  $E_d$  (calculated from the solution in Eqs. (25)),  $E_\pi$  (Eqs. (26)) and  $E_{\text{AF}}$  (Eqs. (27)) represent, respectively, the energy density of the spin-singlet pairing, the spin-triplet pairing, and the AF solutions. The energy of the metallic solution is set to be zero and taken as the energy reference. The interaction strengths used in this plot are the same as those in Fig. 2.

expressions (24) and (25). It is *generic* because the relative sizes of the gaps can be modified by the choice of interaction strengths but their basic forms are dictated entirely by the algebraic structure of the model [and that, in turn, is determined by the physically-motivated choice of generators given in Eq. (3)]. Four doping-dependent energy gaps are predicted:

1. The gap  $\Delta_q$  (Eq. (24a)) measuring antiferromagnetic correlations;  $\Delta_q$  has its maximal value at  $x = 0$ , decreases nearly linearly to the region of the pairing gaps as doping increases, crosses the pairing gaps, and vanishes eventually at the critical doping  $x_q$ .
2. The spin-singlet pairing gap  $\Delta_d$  (Eq. (24b)), which is the superconducting gap for  $x < x_q$ .
3. The spin-singlet pairing gap  $\Delta_0 = \Delta_d$  (Eq. (25b)), which is the superconducting gap for  $x > x_q$  but is not the order parameter for the ground state in the doping range  $x \leq x_q$ .
4. The spin-triplet pairing gap  $\Delta_\pi$  (Eq. (24c)). Similar to the case for  $\Delta_q$ , the triplet gap  $\Delta_\pi$  exists only in the doping range  $x \leq x_q$ . It has its maxi-

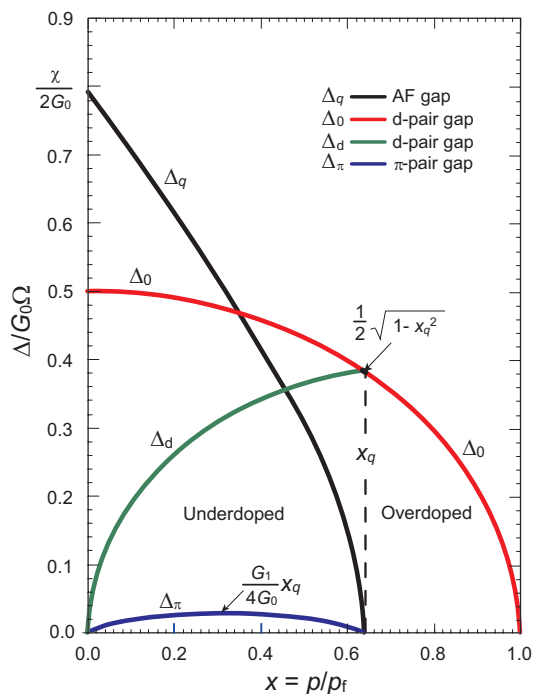


FIG. 2: (Color online) A generic gap diagram for energy gaps versus doping, as predicted by the SU(4) model at  $T = 0$ . The energy gaps are scaled by  $G_0\Omega$  and the doping parameter is scaled by the maximum doping  $P_f$  (We assume  $P_f = 1/4$  [11]). The interaction strengths are assumed to be  $\chi = 13$ ,  $G_0 = 8.2$ , and  $G_1 = 1.3$  (in an arbitrary energy unit), which, according to Eq. (23), requires the critical doping point to be  $x_q = 0.64$ .

mal value at  $x_q/2$  and vanishes at both ends of its range.

Note that the spin-singlet pairing gap exhibits fundamentally different behavior on the left and right sides of  $x_q$ : for  $x > x_q$ , it corresponds to a monotonic curve, labelled as  $\Delta_0$ . However, as the doping decreases from  $x_q$  the spin-singlet gap splits into two curves (labelled as  $\Delta_d$  and  $\Delta_0$ ) having very different doping dependence. Moreover, the splitting correlates strongly with the amount of hole doping: the lower the hole doping, the larger the splitting.

The qualitative features of the SU(4) gap diagram seem to agree with a large body of recent observations in cuprates [2]. In particular, the appearance of a critical doping point and the splitting of the pairing gap in the underdoped compounds are basic predictions of the SU(4) model that have some experimental support [20, 21].

### 1. Critical doping point and pairing gap splitting

The occurrence of a critical doping point and the splitting of the SC pairing gap are understood in the SU(4) model as a direct consequence of competing SC pairing and AF correlation in the doping range below  $x_q$ . When



doping is small the AF correlation dominates the SC pairing. In this case, a state with large AF correlations and suppressed pairing is favored in energy, and thus can become the ground state. Therefore, the SC gap  $\Delta_d$  for the ground state is smaller and the larger pairing gap  $\Delta_0$  is associated with an excited state. However, as doping increases the pairing correlation grows quickly and eventually dominates. The critical doping point  $x_q$  is just the doping fraction at which the AF correlation is completely suppressed.

The critical doping point  $x_q$  defines a natural boundary between *overdoped* and *underdoped* regimes having qualitatively different wavefunctions. It corresponds to the doping point where AF correlations vanish and separates a doping regime characterized by weak superconductivity and reduced pair condensation energy from a doping regime characterized by strong superconductivity and maximal pair condensation. The optimal doping point (corresponding to the maximum of the SC pairing gap) has been used extensively in the literature to mark the boundary between underdoped and overdoped superconductors. It is the doping point where the competition between the AF and SC correlations leads to the maximal  $T_c$ , but our results indicate that it does not mark a boundary between qualitatively different physical regimes characterized by qualitatively different wavefunctions.

According to the SU(4) model, the experimentally observed location of the critical doping point can set a strict constraint on the relative strengths of the three elementary interaction strengths,  $\chi$ ,  $G_0$ , and  $G_1$ . As one can see from Eq. (23),  $\chi$  must be either greater or less than the other two strengths  $G_0$  and  $G_1$ ; otherwise  $(\chi - G_0)/(\chi - G_1)$  would become negative and no  $x_q$  could occur in the physical range  $0 \leq x \leq 1$ . Observations require that  $\chi$  be greater than both  $G_0$  and  $G_1$  in order for the normal state at the half-filling to be an AF state (Mott insulator). It then follows that  $G_0$  should be intermediate in strength between  $\chi$  and  $G_1$ ; otherwise  $(\chi - G_0)/(\chi - G_1) > 1$  will lead to  $x_q > 1$ , which is outside the physical doping range. Thus the SU(4) symmetry and the basic experimental observations require that the three interaction strengths must satisfy the condition  $\chi > G_0 > G_1$ . This is the condition that we have assumed in (22).

It is instructive to examine two extreme cases of Eq. (23): one is  $x_q = 1$  if  $G_0 = G_1$ ; the other is  $x_q = 0$  if  $\chi = G_0$ . For these two cases no critical doping point  $x_q$  exists within the physical doping range. These cases correspond, respectively, to the SO(4) and SO(5) symmetry limits of the SU(4) model, as has been mentioned in Section II. A. For the former case ( $x_q = 1$ ), there is no room for the SC phase at any  $x$ , suggesting that the system in the entire doping range is in the AF phase. For the latter case ( $x_q = 0$ ), the system is in the SO(5) limit. Although the energy minimum in this limit is at  $\Delta_q = 0$ , the same as for the SC case, it is very shallow and the system has large AF and pairing fluctuations.

The SO(5) energy surface at  $x = 0$  is in fact completely flat, develops an energy minimum with  $\Delta_q = 0$  as the doping  $x$  increases, and gradually evolves to an SC-like state at  $x = 1$ . This behavior is characteristic of a critical dynamical symmetry, as discussed extensively in Ref. [10].

## 2. Nature of the pseudogap

The observation of pseudogap behavior in cuprates [1, 2] has motivated a variety of theoretical discussions but there is little agreement on the source of this behavior. Two alternative classes of explanation for the origin of pseudogaps have received considerable attention [2]: (1) The *preformed pair picture* [22], which suggests that the formation of pairs and the condensation of those pairs into a state with long-range order happen on two different energy scales, with the pseudogap being the energy needed to form pairs before pairing condensation. If the pseudogap originates in preformed pairs, it should merge with the pairing gap in the overdoped region. (2) The *competing-order picture* [20], which suggests that the pseudogap is an energy scale associated with a form of order that competes with superconductivity. If the pseudogap originates in competing order, it should not merge with the pairing gap but should instead drop to zero at a critical doping point where the competing order is completely suppressed relative to the superconducting order.

In the solution of the SU(4) gap equations, the resulting energy gaps (scales) are  $\Delta_d$  (as well as  $\Delta_0$ ),  $\Delta_\pi$ , and  $\Delta_q$ . Generally the gaps  $\Delta_d$  and  $\Delta_0$ , may be interpreted as SC gaps and the gaps  $\Delta_\pi$  and  $\Delta_q$  may be interpreted as pseudogaps. However, our results suggest (as mentioned in Section IV.A and discussed further below) that the pure spin-triplet state can neither become a physical ground state at  $T = 0$ , nor be reached by thermal excitations. The  $\Delta_\pi$  gap can coexist with  $\Delta_q$  and  $\Delta_d$  only in underdoped compounds and cannot survive above  $T_c$ . Therefore, within the SU(4) model only the AF gap  $\Delta_q$  is a candidate for the observed pseudogap.

In the competing order picture, the energy scale that competes with superconductivity in cuprates is often identified with antiferromagnetism [20], and this energy scale may be called a pseudogap. The pseudogap energy scale vanishes at the critical doping, which is independent of the disappearance of the SC gap at  $P \approx 0.25$ . Furthermore, experiments have shown (for example, Ref. [20]) that the observed pseudogap is intimately connected with the AF correlations, which disappear exactly at the same critical doping point. The AF gap  $\Delta_q$  has precisely these properties and thus may be interpreted as a pseudogap. Specifically, the scale  $\Delta_q$  in the SU(4) model is the energy per electron required to break the AF correlation. Therefore, the nature of the pseudogap in the SU(4) interpretation is consistent with the competing order picture.

In the SU(4) model the spin-triplet pairing plays a mediating role in the AF–SC competition. As can be seen from Fig. 2, its order parameter  $\Delta_\pi$  is zero at  $x = 0$  where the AF correlations dominate, increases as doping increases to a maximum at half of the critical doping value where the AF and SC correlations are competing strongly, and finally disappears at the critical doping point  $x_q$  where the AF–SC competition ends.

On the other hand, the SU(4) model does not contradict the general preformed pair picture conceptually. If we define preformed pairs as pairs that are formed before pairing condensation, pairs with only AF correlations may be interpreted as preformed pairs. (These AF pairs correspond to a mixture of  $D$  and  $\pi$  pairs in our Hilbert space.) This conclusion will become clear from the discussions later in Section V. Thus  $\Delta_q$  may be viewed also as the scale of stabilization energy associated with preformed pairs that condense into a pure SC pair state only after the AF correlations are completely suppressed by increasing hole doping. A pseudogap arising from this preformed pair picture can exist only in the underdoped regime since  $\Delta_q$  vanishes at the critical doping point. For overdoped systems ( $x > x_q$ ) there is no pseudogap and thus there are no preformed pairs in the gap solutions found here.

### 3. Scaling property of the gaps

It is well known that pairing gaps in cuprates scale with  $(T_c)_{\max}$  (the maximum superconducting transition temperature) for all high- $T_c$  compounds studied so far [23]. According to Ref. [20], there is also strong experimental evidence indicating that the doping value of the putative quantum critical point is universal in the hole-doped cuprates.

In Fig. 2, all the energy gaps are scaled by  $G_0\Omega$ . From Eq. (24b), we know that for any given  $G_0$  the gap  $\Delta_d$  depends only on  $x_q$ . Therefore, if the critical doping point has a universal value the doping dependence of  $\Delta_d$  should also be universal, since we shall show in the next section that  $(T_c)_{\max}$  is proportional to  $G_0$ . The gap  $\Delta_0$  also has this scaling property because, according to Eq. (25b),  $\Delta_0$  in the whole doping range depends only on  $G_0$ .

However, the other two gaps  $\Delta_q$  and  $\Delta_\pi$  do not scale in this way because they depend on  $\chi/G_0$  and  $G_1/G_0$ , respectively. Changing the ratio of  $\chi/G_0$  and  $G_1/G_0$  can change the size of these gaps; thus the doping dependence of  $\Delta_q$  and  $\Delta_\pi$  for different compounds generally could be different. Only if the strength of triplet pairing  $G_1$  is zero (thus  $\Delta_\pi = 0$ ), can  $\Delta_q$  be scaled because in this case

$$\chi/G_0 = 1/(1 - x_q^2).$$

Hence, the scaling property of  $\Delta_q$  may be taken as an indicator of triplet pairing strength in cuprates. Recent  $\Delta_q$  data [20, 24] seem to support such a scaling property, at least approximately, implying that  $G_1/G_0$  should be small.

## V. SOLUTION OF GAP EQUATIONS AT FINITE TEMPERATURES

The gap equations for  $T > 0$  differ from those at  $T = 0$  in that the terms  $w_\pm$  (see Eq. (19)) acquire a temperature dependence

$$w_\pm = \frac{P_\pm(T)}{e_\pm} = \frac{\tanh(Re_\pm/2k_B T)}{e_\pm}. \quad (29)$$

For finite temperature the gap equations could have a variety of solutions, even for a fixed doping  $x$ . Which solution should correspond to the physical ground state depends on temperature and doping, and is determined by minimizing the energy. The solutions that we have derived in Appendix C are obtained under the (physically motivated) condition  $\chi > G_0 > G_1 > 0$ . Under other conditions the gap equations could have different solutions and one has to solve Eqs. (18 – 20) for individual cases.

By comparing the energy densities expressed in Eq. (21), one can then find the solutions having the lowest energy and determine the physical ground-state solution for given temperature  $T$  and doping  $x$ . We examine several cases below.

### A. The $\Delta_d + \Delta_q + \Delta_\pi$ case

This case corresponds to the all-gap solution found at  $T = 0$  for the doping range  $0 \leq x \leq x_q$ . For  $T > 0$ , the temperature and doping dependent gap solutions are derived in Appendix C, with the results

$$\Delta_q = \frac{\chi\Omega}{2} \sqrt{(x_q^{-1} - y)(x_q - y)} \frac{x}{y} \quad (30a)$$

$$\Delta_d = \frac{G_0\Omega}{2} \sqrt{x(x_q^{-1} - y)} g(y) \quad (30b)$$

$$\Delta_\pi = \frac{G_1\Omega}{2} \sqrt{x(x_q - y)} g(y) \quad (30c)$$

$$\lambda' = -\frac{(\chi - G_1)\Omega}{2} x_q \left( \frac{x}{y} - x_q x \right) - \frac{G_1\Omega}{2} x \quad (30d)$$

where  $y$  and  $g(y)$  are defined through

$$y = \frac{x}{\sqrt{I_+(T) + I_-(T)\Gamma(y)}}$$

$$g(y) = \sqrt{\frac{x}{y} + \frac{I_+(T) - (x/y)^2}{2x(\bar{x}_q - y)}}$$

with

$$\Gamma(y) = \frac{\bar{x}_q - y}{\sqrt{(x_q - y)(x_q^{-1} - y)}}$$

$$I_\pm(T) = \frac{P_-^2(T) \pm P_+^2(T)}{2}$$

and  $\bar{x}_q \equiv (x_q^{-1} + x_q)/2$ . It can be verified that these solutions satisfy the SU(4) invariant

$$\langle \mathcal{E}_{\text{SU4}} \rangle = \frac{\Omega^2}{4} [I_+(T) - x^2]. \quad (31)$$

With increasing temperature the system begins to break pairs, with the number density of unpaired particles at temperature  $T$  given by

$$u = 1 - \sqrt{I_+(T)} = 1 - \sqrt{\frac{P_-^2(T) + P_+^2(T)}{2}}. \quad (32)$$

More specifically, to obtain the energy gaps for given doping  $x$  and temperature  $T$ , one may adopt the following procedure. From Eqs. (29) and (16) one obtains

$$T = \frac{R\sqrt{(\Delta_q \pm \lambda')^2 + \Delta_{\pm}^2}}{2k_B \operatorname{atanh}(w_{\pm}e_{\pm})}. \quad (33)$$

This equation implies that

$$\frac{\sqrt{(\Delta_q + \lambda')^2 + \Delta_+^2}}{\operatorname{atanh}(w_+e_+)} = \frac{\sqrt{(\Delta_q - \lambda')^2 + \Delta_-^2}}{\operatorname{atanh}(w_-e_-)}. \quad (34)$$

By solving Eqs. (18c – 18d) directly, one gets

$$w_{\pm} = \frac{\frac{2\Delta_q}{\chi\Omega} \mp x}{\Delta_q \pm \lambda'}.$$

Now by using Eq. (C2) in Appendix C to convert  $\Delta_{\pi}$  into  $\Delta_d$

$$\Delta_{\pi} = \left( \frac{w_- - \omega_0}{w_- - \omega_1} \right) \Delta_d, \quad (35)$$

$\Delta_+$  and  $\Delta_-$  can be related to  $\Delta_d$

$$\Delta_{\pm} = \left[ 1 \pm \left( \frac{w_- - \omega_0}{w_- - \omega_1} \right) \right] \Delta_d. \quad (36)$$

Thus, for a given doping  $x$ , one can solve for  $y$  from Eq. (30a), and  $\lambda'$  from Eq. (30d), for each  $\Delta_q$ . The pairing gap  $\Delta_d$  can then be obtained by solving Eq. (34) directly. With  $\Delta_d$  determined,  $\Delta_{\pi}$  and the corresponding temperature  $T$  can be calculated from Eqs. (35) and (33), respectively.

### B. The $\Delta_d$ case

This case corresponds to one of the trivial solutions at  $T = 0$ . Following a similar procedure as in the  $T = 0$  case, one obtains the temperature and doping dependent gap solutions

$$\Delta_q = \Delta_{\pi} = 0 \quad (37a)$$

$$\Delta_d = \frac{G_0\Omega}{2} \sqrt{I_+(T) - x^2} \quad (37b)$$

$$\lambda' = -\frac{G_0\Omega}{2}x. \quad (37c)$$

Note that in the present case,

$$I_+(T) = P_+^2(T) = P_-^2(T).$$

By using Eqs. (16), (29), and (37c), Eq. (37b) may be written in the following form

$$T = \frac{R\sqrt{\left(\frac{G_0\Omega}{2}x\right)^2 + \Delta_d^2}}{2k_B \operatorname{atanh} \left[ \sqrt{\left(\frac{2\Delta_d}{G_0\Omega}\right)^2 + x^2} \right]}. \quad (38)$$

Therefore, for given  $x$  and  $T$  the gap  $\Delta_d$  can be obtained from Eq. (38), and  $\lambda'$  obtained from (37c).

Since now all the correlations are zero except the spin-singlet pairing, we have

$$\langle \mathcal{E}_{\text{SU4}} \rangle = \langle D^{\dagger}D \rangle = \left( \frac{\Delta_d}{G_0} \right)^2.$$

One can see that the SU(4) invariant (31) is also valid in this case, and the number density of unpaired particles can be evaluated using Eq. (32). It can be checked without difficulty that when  $T \rightarrow 0$ ,

$$P_{\pm}(T) \rightarrow 1 \quad I_+(T) \rightarrow 1,$$

and the solutions (37) then reduce to Eq. (25) of the  $T = 0$  solution.

### C. The $\Delta_q$ case

In this case both  $\Delta_d$  and  $\Delta_{\pi}$  are zero, corresponding to a solution that applies only for temperatures  $T > T_c$ :

$$\Delta_d = \Delta_{\pi} = 0 \quad (39a)$$

$$\Delta_q = \frac{\chi\Omega}{2}(P_-(T) - x). \quad (39b)$$

These results can be derived from Eqs. (18c) and (18d), which in the present case reduce to

$$\frac{4\Delta_q}{\chi\Omega} = P_-(T) + P_+(T), \quad (40)$$

$$2x = P_-(T) - P_+(T). \quad (41)$$

Using Eq. (41), Eq. (39b) can be rewritten as

$$\Delta_q = \frac{\chi\Omega}{2} \sqrt{I_+(T) - x^2}.$$

In a manner similar to that for the  $\Delta_d$  case, one can show that Eqs. (31) and (32) are also valid for the pure AF case ( $\Delta_d = \Delta_{\pi} = 0$ ). Thus Eqs. (31) and (32) are actually general expressions; for different cases only the values of the quasiparticle energies  $e_{\pm}$  (contained in  $P_{\pm}(T)$ ) differ.

By solving Eqs. (40) and (41) one obtains

$$T = \frac{R\Delta_q}{k_B A_+} \quad (42)$$

$$\lambda' = \frac{k_B T A_-}{R}, \quad (43)$$

with

$$A_{\pm} \equiv \left[ \operatorname{atanh} \left( \frac{2\Delta_q}{\chi\Omega} - x \right) \pm \operatorname{atanh} \left( \frac{2\Delta_q}{\chi\Omega} + x \right) \right].$$

Thus, for a temperature  $T$ ,  $\Delta_q$  can be obtained from Eq. (42) and  $\lambda'$  from Eq. (43).

There is an intriguing point concerning the pure AF state at  $T = 0$  that should be clarified. On one hand, when  $T = 0$ , we have that  $P_-(0) = 1$  and  $P_+(0) = 1 - 2x$ . Thus

$$I_+(0) = 1 - 2x + 2x^2,$$

and according to Eq. (32),  $u > 0$ . This means that, if  $x \neq 0$ , the pure AF phase requires pair breaking even at  $T = 0$ . The SU(4) invariant in this case is

$$\langle \mathcal{E}_{\text{SU4}} \rangle = \langle Q^\dagger Q \rangle = \frac{\Omega^2}{4} (1 - x)^2.$$

On the other hand, it is our basic assumption that when  $T = 0$  all particles are paired ( $u = 0$ ) and the SU(4) invariant should be

$$\langle \mathcal{E}_{\text{SU4}} \rangle = \frac{\Omega^2}{4} (1 - x^2),$$

which is state-independent if SU(4) symmetry holds. Despite appearances, these two expressions for  $\langle \mathcal{E}_{\text{SU4}} \rangle$  are not in contradiction because when there exist pairing correlations (one or both of  $G_0$  and  $G_1$  nonzero), no AF state can be the  $T = 0$  ground state unless  $x = 0$ . The only possibility for the pure AF state to become the ground state at  $T = 0$  for  $x > 0$  is in the absence of pairing ( $G_0 = G_1 = 0$ ). But under this condition it is not necessary to require  $\langle D^\dagger D \rangle = \langle \pi^\dagger \pi \rangle = 0$ , so that  $\langle D^\dagger D \rangle$  and  $\langle \pi^\dagger \pi \rangle$  can supplement  $\langle Q^\dagger Q \rangle$  to preserve the invariance  $\langle \mathcal{E}_{\text{SU4}} \rangle = \frac{\Omega^2}{4} (1 - x^2)$ .

## VI. THE PHASE DIAGRAM

We now use the preceding results to construct temperature versus doping phase diagrams in the SU(4) model. The interaction strength parameters of the theory represent effective interactions within a truncated space. For an effective interaction approach to make sense, the interaction strengths cannot have very strong local dependence on global parameters such as doping fraction (except for possible rapid changes at phase boundaries). However, since the effective interaction strengths represent renormalized interactions within a highly truncated

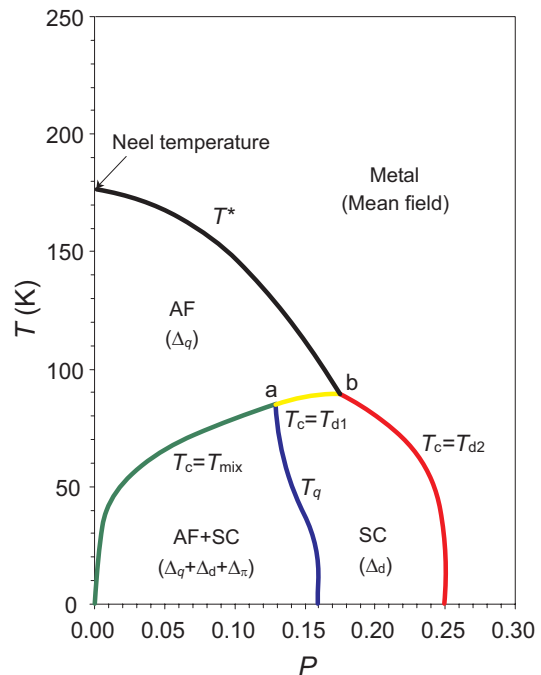


FIG. 3: (Color online) Phase diagram predicted by the SU(4) model with  $R = 0.6$ . The interaction strengths are the same as those used in Fig. 2, but in units of  $k_B(T_c)_{\max}$ , where  $(T_c)_{\max}$  is taken to be 90 K. The two points marked as  $a$  and  $b$  are tricritical points. The critical doping point is at  $P_q = 0.16$  (corresponding to  $x_q = 0.64$ ).

space, they may reasonably be expected to have a smooth dependence on the global parameters. Nevertheless, it is useful to make the simplest assumption for a starting point: the effective interaction strengths are *constant* across the entire doping range relevant to cuprates. Although this is a more stringent restriction than is warranted for a realistic theory, it has the advantage of simplicity and it should give at least sensible qualitative results if the present approach is valid.

In Fig. 3 we show a typical phase diagram. In the calculations the interaction strengths are kept constant, with the same values as those in the zero-temperature case discussed in Figs. 1 and 2. The only adjustable parameter is  $R$  (appearing in Eq. (11)), the energy scaling parameter that approximately corrects for the possible error caused by the degeneracy assumption in the quasiparticle excitation spectrum for a finite  $T$ .

There are four distinct phases emerging in Fig. 3: a pure antiferromagnetic phase (AF), a superconducting phase (SC), a transitional phase with all three correlations present, which may be called a mixed phase (marked as AF+SC), and a metallic phase. The correlations (energy gaps) associated with each phase are indicated in parentheses. The doping-dependent transition temperatures  $T_c$ ,  $T^*$ , and  $T_q$  define the boundaries for these phases. There are two tricritical points  $a$  and  $b$ , which are the intersection points of three phases.

### A. Phases below the critical temperature

We first discuss the phases below the critical temperature  $T_c$ . In the phase diagram of Fig. 3 there are two phases below  $T_c$ , the mixed phase and the SC phase. The essential difference between them is that the mixed phase has both AF correlation  $\Delta_q$  and triplet pairing  $\Delta_\pi$  mixed with the singlet pairing  $\Delta_d$ , while the SC phase has a pure  $\Delta_d$  correlation with  $\Delta_q = \Delta_\pi = 0$ . At zero temperature, the separation point between these two phases corresponds to the critical doping point  $x_q$ .

The boundary between the mixed phase and the SC phase is marked in Fig. 3 as  $T_q$ , which is the locus of all points where the corresponding energies of the two phases are equal

$$\frac{[\Delta_d^{(2)}(T_q)]^2}{G_0} = \frac{[\Delta_d^{(1)}(T_q)]^2}{G_0} + \frac{[\Delta_\pi^{(1)}(T_q)]^2}{G_1} + \frac{[\Delta_q^{(1)}(T_q)]^2}{\chi}. \quad (44)$$

Here we use the superscript indices ‘(1)’ and ‘(2)’ to distinguish quantities evaluated in the mixed and SC phases, respectively.

Eq. (44) indicates that the order parameters  $\Delta_d$ ,  $\Delta_\pi$ , and  $\Delta_q$  could be discontinuous across the boundary except for  $T = 0$ . This implies that the mixed–SC phase transition is second-order at  $T = 0$ , but could generally be first-order for finite  $T$ . The actual situation depends on the relative location of the critical points  $a$ ,  $b$ , and  $x_q$ . Using  $P_\sigma$  (or  $x_\sigma$ ) with  $\sigma = a$  or  $b$  to represent doping fractions corresponding to the tricritical points, we can show that the transition is indeed first-order if  $x_q < x_b$ , as illustrated in Fig. 3.

Quite interestingly, if  $x_q \geq x_b$  the point  $a$  merges with the point  $b$ , as illustrated in Fig. 4. The point  $b$  is now a quadracritical point, where at this unique doping and temperature *all four* phases that we have identified in the SU(4) model can coexist in equilibrium with each other. In this case, all the order parameters change smoothly across the boundary and the mixed–SC phase transition becomes second-order. The curve  $T_q$  in this case looks like an extension of the curve for transition temperature  $T^*$ . The results in Fig. 4 are obtained for a larger  $x_q$  value than for those in Fig. 3. This suggests that the precise value of the critical doping point is related to the number of tricritical points in the phase diagram and to the order of the phase transitions.

Both results presented in Figs. 3 and 4 are possible solutions. The only difference between them is the triplet pairing strength  $G_1$ . In Fig. 3,  $G_1 = 1.3$  is used, resulting in a smaller  $x_q = 0.64$ , while in Fig. 4,  $G_1 = 4.7$  corresponding to  $x_q = 0.76$ . The former case has  $x_q < x_b$  and the latter  $x_q > x_b$ . This suggests that the relative position of  $x_q$  and  $x_b$  could be an indicator of the strength of triplet pairing. It would be extremely interesting to confirm experimentally whether the real phase diagram in cuprates is of the Fig. 3 or Fig. 4 type.

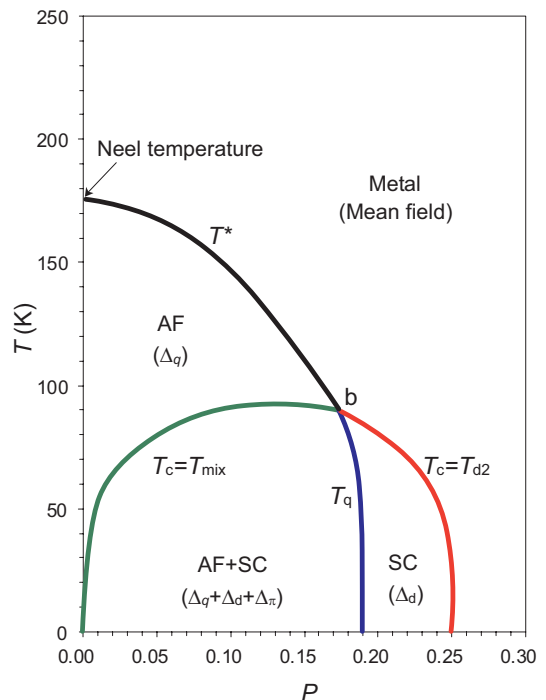


FIG. 4: (Color online) Phase diagram predicted by the SU(4) model for  $P_q > P_b$ .  $P_q = 0.19$  (corresponding to  $x_q = 0.76$ ) is chosen in this figure while  $P_b = 0.175$  (corresponding to  $x_q = 0.7$ ) is the same as that in Fig. 3. All the parameters remain unchanged except that  $G_1$  increases from 1.3 to 4.7 (in units of  $k_B(T_c)_{\max}$ ) for a larger  $P_q$  value.

### B. The critical temperature

Let us use Fig. 3 to discuss the critical temperature  $T_c$ . The curve for  $T_c$  in the SU(4) phase diagram consists of three segments:

$$T_c = \begin{cases} T_{\text{mix}} & (P \leq P_a) \\ T_{\text{d1}} & (P_a < P < P_b) \\ T_{\text{d2}} & (P \geq P_b) \end{cases},$$

which are seen to behave quite differently. The discussions below apply also to Fig. 4 because in this case there is only one phase boundary intersection point  $b$  and thus the segment  $T_{\text{d1}}$  does not exist.

In the doping range  $P \geq P_b$  the critical temperature is  $T_c = T_{\text{d2}}$ , which is the SC–metal transition temperature and can be expressed analytically using Eq. (38) with  $\Delta_d = 0$ :

$$\begin{aligned} T_c &= T_{\text{d2}} = T(\text{SC} \leftrightarrow \text{metal}) \\ &= G_0 \Omega \frac{Rx}{4k_B \operatorname{atanh}(x)} \quad (x \geq x_b). \end{aligned} \quad (45)$$

In the doping range  $P \leq P_a$  the critical temperature is  $T_c = T_{\text{mix}}$ , which is the mixed–AF transition temperature determined from Eq. (33) with  $\Delta_d = 0$  (thus

$\Delta_{\pm} = 0$ ):

$$\begin{aligned} T_c &= T_{\text{mix}} = T(\text{mixed} \leftrightarrow \text{AF}) \\ &= \frac{R|\Delta_q \pm \lambda'|}{2k_B \operatorname{atanh}\left(\frac{2\Delta_q}{\chi\Omega} \mp x\right)} \quad (x \leq x_a), \end{aligned} \quad (46)$$

where  $\lambda'$  depends on  $\Delta_q$  through  $y$  [see Eqs. (30a) and (30d)] and  $\Delta_q$  is determined by Eq. (34).

In the doping range  $P_a < P < P_b$  the critical temperature is  $T_c = T_{\text{d1}}$ , which is the SC–AF phase boundary and determined by the condition that at  $T_c$  the energies of the two phases are equal:

$$\frac{[\Delta_d(T_c)]^2}{G_0} = \frac{[\Delta_q(T_c)]^2}{\chi}. \quad (47)$$

Using this condition and Eqs. (38) and (42), one can obtain the pairing gap  $\Delta_d$  through the following equation

$$\begin{aligned} &\frac{\sqrt{\left(\frac{G_0\Omega}{2}x\right)^2 + \Delta_d^2}}{2 \operatorname{atanh}\left[\frac{2}{G_0\Omega}\sqrt{\left(\frac{G_0\Omega}{2}x\right)^2 + \Delta_d^2}\right]} = \\ &\frac{\sqrt{\chi/G_0}\Delta_d}{\operatorname{atanh}\left(\frac{2\Delta_d}{\sqrt{\chi}G_0\Omega} - x\right) + \operatorname{atanh}\left(\frac{2\Delta_d}{\sqrt{\chi}G_0\Omega} + x\right)} \end{aligned}$$

and  $T_c$  is then determined by the equation

$$\begin{aligned} T_c &= T_{\text{d1}} = T(\text{SC} \leftrightarrow \text{AF}) \\ &= \frac{R\sqrt{\left(\frac{G_0\Omega}{2}x\right)^2 + \Delta_d^2}}{2k_B \operatorname{atanh}\left[\sqrt{\left(\frac{2\Delta_d}{G_0\Omega}\right)^2 + x^2}\right]}, \end{aligned} \quad (48)$$

which is valid in the doping range  $x_a \leq x \leq x_b$ .

The phase transitions in the two regions ( $P \leq P_a$  and  $P \geq P_b$ ) are second-order (all gaps change smoothly across the boundary). However, transitions in the range  $x_a \leq x \leq x_b$  behave very differently. The pairing gap  $\Delta_d$  in this doping range drops discontinuously to zero when crossing the boundary, while the AF gap  $\Delta_q$  jumps from zero to a finite value, suggesting that the system undergoes a first-order phase transition from the SC to AF phase.

In traditional BCS theory the energy gap appearing in the density of states is identified with the pairing gap. This remains true for the overdoped regime ( $T_{\text{d2}}$ ) where the singlet pairing is the only correlation. However, this is *not true* for underdoped systems where more correlations are involved and a pairing gap is not necessarily equivalent to the energy gap appearing in the density of

states. As shown in Eq. (16), in the underdoped regime with the mixed phase there are two gaps,  $\Delta_{\pm}$ , in the density of states, but neither of them is an order parameter. The actual process of the mixed–AF transition is as follows: with increasing temperature,  $\Delta_{\pi} \rightarrow 0$  at a temperature that causes  $w_- = w_0$  before  $T_c$  is reached [see Eqs. (35 – 36)], and at this temperature  $\Delta_{\pm}$  reduce to  $\Delta_d$ . After that, the order parameter  $\Delta_d \rightarrow 0$  at  $T_c$ .

This complexity in gap structure suggests that one has to be careful with the interpretation of energy gaps measured in underdoped compounds. According to the SU(4) model, there are several gaps involved in this doping and temperature range such as  $\Delta_d$ ,  $\Delta_0$ ,  $\Delta_{\pi}$ ,  $\Delta_+$ , and  $\Delta_-$ , and they all can correspond to energy scales having the same order of magnitude. Therefore, an energy gap by two different experimental probes may not really be the same gap since a particular measurement may be sensitive only to certain of these gaps because of their microscopic structure.

The location of the tricritical point  $x_a$  can be determined from  $T_{\text{mix}}(x_a) = T_{\text{d1}}(x_a)$  with the condition that the energies of the mixed and SC phases at this point are equivalent. By using Eqs. (46) and (48),  $x_a$  can be obtained by solving the following equations

$$\frac{|\Delta_q \pm \lambda'|}{\operatorname{atanh}\left(\frac{2\Delta_q}{\chi\Omega} \mp x_a\right)} = \frac{\sqrt{\left(\frac{G_0\Omega}{2}x_a\right)^2 + \Delta_d^2}}{\operatorname{atanh}\left(\sqrt{\left(\frac{2\Delta_d}{G_0\Omega}\right)^2 + x_a^2}\right)}$$

where  $\Delta_q$  and  $\lambda'$  are known if  $T_{\text{mix}}$  is determined, while  $\Delta_d$  is calculated through the condition  $\Delta_q^2/\chi = \Delta_d^2/G_0$ .

### C. Phases above the critical temperature

For temperatures above  $T_c$  there are two possible phases: the pure AF phase and the metallic phase.

As already mentioned, the pure AF phase at  $T = 0$  can exist only at  $x = 0$  as a limit of the mixed phase. This is because of pairing correlations that give the mixed phase a more favorable energy, and is qualitatively consistent with the observation that the AF phase is favored only in a very restricted doping region near half filling.

When  $T > T_c$ , however, the pure AF phase can become the ground state in the underdoped regime, as predicted in Fig. 3. This is because thermal fluctuations can destroy the pairing correlations preferentially relative to the AF correlations. If temperature increases further, the AF correlation will eventually be totally destroyed ( $\Delta_q \rightarrow 0$ ) and the system will undergo an AF–metal transition.

The AF–metal transition is second-order. The transition temperature  $T^*$  is determined by Eq. (42) in the

limit that  $\Delta_q \rightarrow 0$ :

$$\begin{aligned} T^* &= T(\text{AF} \leftrightarrow \text{metal}) \\ &= \frac{R\chi\Omega(1-x^2)}{4k_B} \quad (0 \leq x \leq x_b). \end{aligned} \quad (49)$$

The Néel temperature can be determined from the preceding equation with  $x = 0$ ,

$$T_N = \frac{R\chi\Omega}{4k_B} \quad (x = 0).$$

The location of tricritical point  $x_b$  can be determined through the condition  $T_{d2}(x_b) = T^*(x_b)$ . Combining Eq. (49) with (45) gives

$$x_b = \sqrt{1 - \frac{G_0}{\chi} \frac{x_b}{\text{atanh}(x_b)}}.$$

#### D. Discrepancies

The phase diagrams of the SU(4) model are consistent with much of the current understanding for cuprate systems. However, there are two obvious quantitative discrepancies between the simplified results presented here and data.

One discrepancy occurs at very low doping. Data show that the pure AF phase is not confined to half filling but can extend over a narrow non-zero doping range at low temperature. Experimentally,  $T_c$  goes to zero at  $P \approx 0.05$ , which differs from the theoretical prediction  $P = 0$ . However, recall that we have deliberately employed an oversimplified model here (effective interactions independent of doping) in order to emphasize that the qualitative features of the SU(4) quasiparticle solution follow from the physics encoded in the algebraic structure, not from detailed parameter adjustment. As we have shown, in the SU(4) model the condition for the pure AF state to be the ground state is the complete absence of pairing interactions. Since we have assumed all effective interaction strengths to be constant over the whole doping range, the pairing correlation exists at all dopings. This is not a favorable condition for the AF phase to be the ground state and with these assumptions  $T_c$  can go to zero only at the both ends of the doping range,  $x = 0$  ( $P = 0$ ) and  $x = 1$  ( $P = 0.25$ ). This discrepancy suggests that there exists an onset of effective pairing correlation around  $P_i \approx 0.05$ . If we allow a simple variation of pairing strength with doping implying that the pairs become stable and thus have pairing correlation only when  $P > P_i$ , this discrepancy can be resolved easily.

A second quantitative discrepancy is that our predicted Néel temperature is too low (175 K) for a cuprate system with  $(T_c)_{\text{max}} \approx 90$  K. Again, if we relax the assumption of constant interaction strength by considering different AF correlation strength  $\chi$  before and after the onset of

pairing near  $P = 0.05$  (for example, maximal  $\chi$  at  $x = 0$  that decreases as doping increases and finally is stabilized at a smaller value when pairing is established), this problem is also easy to resolve. Work to establish the mechanism for pair formation and thereby to quantify the expected doping dependence of the effective interactions is in progress and details will be reported elsewhere.

#### VII. SUMMARY

The present work has used dynamical symmetries, Lie algebras, and generalized coherent states to derive the temperature-dependent gap equations expected for a theory in which antiferromagnetism and  $d$ -wave superconductivity compete on an equal footing, and for which the normal undoped states have Mott insulator character. Although the SU(4) model is constructed using symmetry principles, the coherent state method permits the problem to be cast in the form of a generalized quasiparticle problem. Therefore, the results are presented in terms of equations that may be recognized as a generalization of the BCS formalism to include more than one kind of pairing, subject to an SU(4) symmetry constraint. This symmetry constraint has a clear physical origin. As the preceding discussion has shown, SU(4) symmetry may be viewed as concise shorthand for competing antiferromagnetism and  $d$ -wave superconductivity on a 2-dimensional lattice with no double occupancy.

The quasiparticle structure that results for the cuprate superconductors is rather rich, giving rise to novel gap structures including both pairing gaps and pseudogaps, and a potentially complex phase diagram. A critical doping point  $P_q$  appears naturally in the theory as the boundary between doping regimes having qualitatively different ground-state wavefunctions at zero temperature: a pure superconducting solution at higher doping ( $P > P_q$ ) and a solution with superconductivity strongly suppressed by antiferromagnetism at lower doping ( $P < P_q$ ). Thus, the critical doping point is associated with a quantum phase transition. The pairing gap has been shown to have two solutions for  $P < P_q$ : a small gap, associated with competition between superconductivity and antiferromagnetism that is responsible for the ground-state superconductivity in underdoped systems, and a large gap without antiferromagnetic suppression that corresponds to a collective excited pairing state.

Within the SU(4) model a pseudogap can occur naturally. It has been demonstrated that the pseudogap originates from the competition of antiferromagnetism with  $d$ -wave superconductivity in the underdoped regime, and terminates exactly at the critical doping point. These conclusions are in accord with many current observations in cuprates. Although the pseudogap arises directly from competing antiferromagnetic and superconducting order, we have also argued that it may be interpreted in a preformed pair picture since the corresponding wavefunction contains singlet and triplet pairs fluctuating in an antifer-

romagnetic background but no long-range pairing order.

Once the parameters in the SU(4) gap diagram are determined by fitting to the gap data, a rich phase diagram as a function of temperature and doping can be sketched with only one additional adjustable parameter. A variety of phases reflecting the interplay of the spin-singlet and spin-triplet pairing with the antiferromagnetic correlations has been predicted. Properties of the phases may be expressed quantitatively using the mathematical properties of the SU(4) algebra and its coherent states, leading to a set of testable predictions concerning phase structure and phase transitions in the cuprate superconductors.

Finally, we note that the striking properties in the phase diagram discussed in this paper have similarities with properties observed in other materials (often at lower temperature and energy scales). For example, in heavy-fermion compounds and some 2D organic superconductors a superconducting phase appears near the boundary of an AF phase. As a second example, the manganites have complex competing phases, some bearing a resemblance to those discussed in this paper. Therefore, we expect that the general formalism presented here, which is uniquely suited to deal quantitatively with multiple competing low-temperature phases in strongly correlated systems, will prove applicable to a much broader range of systems with doping replaced or supplemented by additional control parameters such as pressure or strength of magnetic field.

### Acknowledgments

We are grateful for useful discussions with G. Arnold, E. Dagatto, P.-C. Dai, T. Egami, B. Fine, T. K. Lee, A. Moreo, C.-Y. Mou, T. Papenbrock, and H.-H. Wen.

### APPENDIX A: MATRIX REPRESENTATION OF THE SU(4) ALGEBRA

To facilitate the evaluation of  $\delta\langle H' \rangle = 0$  in section III.A, it is convenient to use a matrix representation introduced in Ref. [10, 19]. In this representation the SU(4) generators are expressed in terms of  $4 \times 4$  matrices, with the matrix elements defined in the following 4-dimensional single-particle basis:

$$\{c_{\mathbf{r}\uparrow}^\dagger|0^*\rangle, c_{\mathbf{r}\downarrow}^\dagger|0^*\rangle, c_{\mathbf{r}\uparrow}|0^*\rangle, c_{\mathbf{r}\downarrow}|0^*\rangle\}.$$

Explicitly, for an operator  $\hat{O}$  this is implemented through the following mapping:

$$\begin{aligned} \begin{bmatrix} O^{11} & O^{12} \\ O^{21} & O^{22} \end{bmatrix} &\Rightarrow \hat{O} = \sum_{\mathbf{r}, i, j} \left[ O_{ij}^{(11)} c_{\mathbf{r}i}^\dagger c_{\mathbf{r}j} + O_{ij}^{(22)} c_{\mathbf{r}i} c_{\mathbf{r}j}^\dagger \right. \\ &\quad \left. + O_{ij}^{(12)} c_{\mathbf{r}i}^\dagger c_{\mathbf{r}j}^\dagger + O_{ij}^{(21)} c_{\mathbf{r}i} c_{\mathbf{r}j} \right], \end{aligned} \quad (\text{A1})$$

where  $O^{kl}$  ( $k, l = 1$  or  $2$ ) are  $2 \times 2$  matrices with matrix elements  $O_{ij}^{(kl)}$ . A 4-dimensional faithful matrix representation of SU(4) generators (8) can be obtained immediately from this mapping:

$$\begin{aligned} p_{12}^\dagger &= \begin{bmatrix} 0 & i\sigma_y \\ 0 & 0 \end{bmatrix} & p_{12} &= \begin{bmatrix} 0 & 0 \\ -i\sigma_y & 0 \end{bmatrix} \\ q_{12}^\dagger &= \begin{bmatrix} 0 & \sigma_x \\ 0 & 0 \end{bmatrix} & q_{12} &= \begin{bmatrix} 0 & 0 \\ \sigma_x & 0 \end{bmatrix} \\ q_{11}^\dagger &= \begin{bmatrix} 0 & I + \sigma_z \\ 0 & 0 \end{bmatrix} & q_{11} &= \begin{bmatrix} 0 & 0 \\ I + \sigma_z & 0 \end{bmatrix} \\ q_{22}^\dagger &= \begin{bmatrix} 0 & I - \sigma_z \\ 0 & 0 \end{bmatrix} & q_{22} &= \begin{bmatrix} 0 & 0 \\ I - \sigma_z & 0 \end{bmatrix} \\ S_{12} &= \begin{bmatrix} \sigma_+ & 0 \\ 0 & -\sigma_- \end{bmatrix} & S_{21} &= \begin{bmatrix} \sigma_- & 0 \\ 0 & -\sigma_+ \end{bmatrix} \\ S_{11} &= \begin{bmatrix} \frac{I+\sigma_z}{2} & 0 \\ 0 & -\frac{I+\sigma_z}{2} \end{bmatrix} & S_{22} &= \begin{bmatrix} \frac{I-\sigma_z}{2} & 0 \\ 0 & -\frac{I-\sigma_z}{2} \end{bmatrix} \\ \tilde{Q}_{12} &= \begin{bmatrix} \sigma_+ & 0 \\ 0 & \sigma_- \end{bmatrix} & \tilde{Q}_{21} &= \begin{bmatrix} \sigma_- & 0 \\ 0 & \sigma_+ \end{bmatrix} \\ \tilde{Q}_{11} &= \begin{bmatrix} \frac{I+\sigma_z}{2} & 0 \\ 0 & \frac{I+\sigma_z}{2} \end{bmatrix} & \tilde{Q}_{22} &= \begin{bmatrix} \frac{I-\sigma_z}{2} & 0 \\ 0 & \frac{I-\sigma_z}{2} \end{bmatrix} \end{aligned} \quad (\text{A2})$$

where  $\sigma_x, \sigma_y$ , and  $\sigma_z$  are Pauli matrices in the standard representation,  $\sigma_\pm \equiv \frac{1}{2}(\sigma_x \pm i\sigma_y)$ , and  $I$  is a unit matrix. A corresponding matrix representation of the operators (3) is then constructed readily from Eq. (A2). The unitary transformation operator  $\mathcal{T}$  of Eq. (9) may be written in this matrix representation as

$$\mathcal{T} = \begin{bmatrix} \mathbf{Y}_1 & \mathbf{X} \\ -\mathbf{X}^\dagger & \mathbf{Y}_2 \end{bmatrix}, \quad (\text{A3})$$

with the definitions

$$\mathbf{X} = \begin{bmatrix} 0 & v_+ \\ -v_- & 0 \end{bmatrix} \quad \mathbf{Y}_1 = \begin{bmatrix} u_+ & 0 \\ 0 & u_- \end{bmatrix} \quad \mathbf{Y}_2 = \begin{bmatrix} u_- & 0 \\ 0 & u_+ \end{bmatrix},$$

where the requirement of unitarity implies that

$$u_\pm^2 + v_\pm^2 = 1.$$

The  $u$ 's and  $v$ 's are variational parameters in the matrix representation and are related to the parameters  $\eta_{00}$  and  $\eta_{10}$  in Eq. (10).

The Bogoliubov-type transformation (A3) applied to the  $D-\pi$  pair space may be viewed as a quasiparticle transformation that is further constrained to preserve the SU(4) symmetry. The physical vacuum state  $|0^*\rangle$  is transformed to a quasiparticle vacuum state  $|\psi\rangle$  and the basic fermion operators,

$$\{c_{\mathbf{r}\uparrow}^\dagger, c_{\mathbf{r}\downarrow}^\dagger, c_{\mathbf{r}\uparrow}, c_{\mathbf{r}\downarrow}\},$$

are converted to quasifermion operators,

$$\{a_{\mathbf{r}\uparrow}^\dagger, a_{\mathbf{r}\downarrow}^\dagger, a_{\mathbf{r}\uparrow}, a_{\mathbf{r}\downarrow}\} \quad \text{with} \quad a_{\mathbf{r}i}|\psi\rangle = 0,$$



through the transformation

$$\mathcal{T} \begin{pmatrix} c_{\mathbf{r}\uparrow} \\ c_{\mathbf{r}\downarrow} \\ c_{\bar{\mathbf{r}}\uparrow} \\ c_{\bar{\mathbf{r}}\downarrow} \end{pmatrix} |0^*\rangle = \begin{pmatrix} a_{\mathbf{r}\uparrow} \\ a_{\mathbf{r}\downarrow} \\ a_{\bar{\mathbf{r}}\uparrow} \\ a_{\bar{\mathbf{r}}\downarrow} \end{pmatrix} |\psi\rangle. \quad (\text{A4})$$

Using the transformation (A4) and the mapping (A1), one can express any one-body operator in the quasiparticle space as

$$\begin{aligned} \mathcal{T}\hat{O}\mathcal{T}^{-1} &= \begin{bmatrix} \mathcal{O}^{(11)} & \mathcal{O}^{(12)} \\ \mathcal{O}^{(21)} & \mathcal{O}^{(22)} \end{bmatrix} \\ \Rightarrow \hat{O} &= \sum'_{\mathbf{r},i} \mathcal{O}_{ii}^{(22)} + \sum'_{\mathbf{r},i,j} \left\{ \mathcal{O}_{ij}^{(11)} a_{\mathbf{r}i}^\dagger a_{\mathbf{r}j} - \mathcal{O}_{ji}^{(22)} a_{\bar{\mathbf{r}}i}^\dagger a_{\bar{\mathbf{r}}j} \right. \\ &\quad \left. + \mathcal{O}_{i,j}^{(12)} a_{\mathbf{r}i}^\dagger a_{\bar{\mathbf{r}}j} + \mathcal{O}_{i,j}^{(21)} a_{\bar{\mathbf{r}}i} a_{\mathbf{r}j} \right\}, \end{aligned} \quad (\text{A5})$$

where we put a prime on the summation symbols to indicate that the summation runs only over  $\mathbf{r} \in$  even lattice sites. The  $\mathcal{O}_{ij}^{(\mu\nu)}$  are fixed by the transformation properties of the operator  $\hat{O}$ :

$$\mathcal{O}_{ij}^{(\mu\nu)} = \sum'_{m,n} [\mathcal{T}^{(\mu m)} \mathcal{O}^{(mn)} (\mathcal{T}^{-1})^{(n\nu)}]_{ij}, \quad (\text{A6})$$

and  $\mathcal{T}^{(\mu m)}$  and  $\mathcal{O}^{(mn)}$  are two-dimensional submatrices of  $\mathcal{T}$  and  $\hat{O}$ , respectively.

Because the quasiparticle annihilation operator acting on the quasiparticle vacuum  $|\psi\rangle$  gives zero, the expectation values for one-body operators  $\hat{O}$  are given by

$$\langle \hat{O} \rangle = \langle \psi | \hat{O} | \psi \rangle = \sum'_{\mathbf{r},i} \mathcal{O}_{ii}^{(22)} = \sum'_{\mathbf{r}} \text{Tr}(\mathcal{O}^{(22)}), \quad (\text{A7})$$

and for two-body operators  $\hat{O}_A \hat{O}_B$ ,

$$\begin{aligned} \langle \hat{O}_A \hat{O}_B \rangle &= \langle \psi | \hat{O}_A \hat{O}_B | \psi \rangle \\ &= \sum'_{\mathbf{r}} \text{Tr}(\mathcal{O}_A^{(22)}) \sum'_{\mathbf{r}'} \text{Tr}(\mathcal{O}_B^{(22)}) \\ &\quad + \sum'_{\mathbf{r}} \text{Tr}(\mathcal{O}_A^{(21)} \mathcal{O}_B^{(12)}). \end{aligned} \quad (\text{A8})$$

Utilizing Eqs. (A3) and (A6)–(A8), and noting that the summation  $\sum'_{\mathbf{r}}$  provides a factor of  $\Omega/2$  because the matrix elements of Eq. (A6) do not depend on  $\mathbf{r}$ , one obtains the expectation values for the SU(4) generators and their scalar products in the coherent state representation. For one-body terms,

$$\begin{aligned} \langle D^\dagger \rangle &= \langle D \rangle = -\frac{\Omega}{2}(u_+ v_+ + u_- v_-) \\ \langle \pi_z^\dagger \rangle &= \langle \pi_z \rangle = -\frac{\Omega}{2}(u_+ v_+ - u_- v_-) \\ \langle \mathcal{Q}_z \rangle &= \frac{\Omega}{2}(v_+^2 - v_-^2) \\ \langle \hat{n} \rangle &= \Omega(v_+^2 + v_-^2) \\ \langle \pi_x \rangle &= \langle \pi_y \rangle = \langle \vec{S} \rangle = \langle \mathcal{Q}_x \rangle = \langle \mathcal{Q}_y \rangle = 0, \end{aligned} \quad (\text{A9})$$

and for two-body terms

$$\begin{aligned} \langle D^\dagger D \rangle &= \langle D \rangle^2 = \frac{1}{4}\Omega^2(u_+ v_+ + u_- v_-)^2 \\ \langle \vec{\pi}^\dagger \cdot \vec{\pi} \rangle &= \langle \pi_z \rangle^2 = \frac{1}{4}\Omega^2(u_+ v_+ - u_- v_-)^2 \\ \langle \vec{\mathcal{Q}} \cdot \vec{\mathcal{Q}} \rangle &= \langle \mathcal{Q}_z \rangle^2 = \frac{1}{4}\Omega^2(v_+^2 - v_-^2)^2 \\ \langle \vec{S} \cdot \vec{S} \rangle &= 0, \end{aligned} \quad (\text{A10})$$

where we have applied a large- $\Omega$  approximation, ignoring terms that are of order  $1/\Omega$  smaller than the leading terms. Under this approximation, the expectation value for a two-body operator is simply a product of the expectation values of two one-body operators (that is, the last term on the right side of Eq. (A8) is negligible).

## APPENDIX B: DERIVATION OF THE TEMPERATURE-DEPENDENT GAP EQUATIONS

The formulas in Appendix A are valid only at zero temperature. In this Appendix we extend the derivation to the finite temperature case. Let us begin with a more general Hamiltonian, assuming that the single-particle energies are degenerate only for adjacent sites:

$$\begin{aligned} H &= \sum_{r=\text{even}} \varepsilon_r \hat{n}_r - (G_0 D^\dagger D + G_1 \vec{\pi}^\dagger \cdot \vec{\pi} \\ &\quad + \chi \vec{\mathcal{Q}} \cdot \vec{\mathcal{Q}} + \kappa \vec{S} \cdot \vec{S}), \end{aligned} \quad (\text{B1})$$

where

$$\hat{n}_r \equiv c_{\mathbf{r}\uparrow}^\dagger c_{\mathbf{r}\uparrow} + c_{\bar{\mathbf{r}}\downarrow}^\dagger c_{\bar{\mathbf{r}}\downarrow} + c_{\mathbf{r}\downarrow}^\dagger c_{\mathbf{r}\downarrow} + c_{\bar{\mathbf{r}}\uparrow}^\dagger c_{\bar{\mathbf{r}}\uparrow}.$$

This Hamiltonian is not an invariant with respect to the SU(4) symmetry generated by the operators of Eq. (8). However, with a slight revision, the following 16 operators form a U(4) algebra denoted as  $U_4(\mathbf{r})$  (with an  $SU_4(\mathbf{r})$  subgroup),

$$\begin{aligned} p_{12}^\dagger(\mathbf{r}) &= \left( c_{\mathbf{r}\uparrow}^\dagger c_{\bar{\mathbf{r}}\downarrow}^\dagger - c_{\bar{\mathbf{r}}\downarrow}^\dagger c_{\mathbf{r}\uparrow}^\dagger \right) \\ q_{ij}^\dagger(\mathbf{r}) &= \left( c_{\mathbf{r},i}^\dagger c_{\bar{\mathbf{r}},j}^\dagger + c_{\bar{\mathbf{r}},j}^\dagger c_{\mathbf{r},i}^\dagger \right) \\ S_{ij}(\mathbf{r}) &= \left( c_{\mathbf{r},i}^\dagger c_{\mathbf{r},j} - c_{\bar{\mathbf{r}},j}^\dagger c_{\bar{\mathbf{r}},i}^\dagger \right) \\ \tilde{Q}_{ij}(\mathbf{r}) &= \left( c_{\mathbf{r},i}^\dagger c_{\mathbf{r},j} + c_{\bar{\mathbf{r}},j}^\dagger c_{\bar{\mathbf{r}},i}^\dagger \right) \\ p_{12}(\mathbf{r}) &= \left( p_{12}^\dagger(\mathbf{r}) \right)^\dagger \quad q_{ij}(\mathbf{r}) = \left( q_{ij}^\dagger(\mathbf{r}) \right)^\dagger \end{aligned}$$

with

$$\begin{aligned} p_{12}^\dagger &= \sum_{r=\text{even}} p_{12}^\dagger(\mathbf{r}) & p_{12} &= \sum_{r=\text{even}} p_{12}(\mathbf{r}) \\ q_{ij}^\dagger &= \sum_{r=\text{even}} q_{ij}^\dagger(\mathbf{r}) & q_{ij} &= \sum_{r=\text{even}} q_{ij}(\mathbf{r}) \\ \tilde{Q}_{ij} &= \sum_{r=\text{even}} \tilde{Q}_{ij}(\mathbf{r}) & S_{ij} &= \sum_{r=\text{even}} S_{ij}(\mathbf{r}). \end{aligned}$$

As for Eq. (3), one can also define more physical operators  $D(\mathbf{r})$ ,  $\vec{\pi}(\mathbf{r})$ ,  $\vec{Q}(\mathbf{r})$ ,  $\vec{S}(\mathbf{r})$ ,  $M(\mathbf{r})$ , and  $\hat{n}_r = 2M(\mathbf{r}) + 2$ , and express them as

$$\begin{aligned} D &= \sum_{r=\text{even}} D(\mathbf{r}) & \vec{\pi} &= \sum_{r=\text{even}} \vec{\pi}(\mathbf{r}) \\ \vec{Q} &= \sum_{r=\text{even}} \vec{Q}(\mathbf{r}) & \vec{S} &= \sum_{r=\text{even}} \vec{S}(\mathbf{r}) \\ M &= \sum_{r=\text{even}} M(\mathbf{r}). \end{aligned}$$

The Hamiltonian (B1) has the symmetry of the direct product of  $SU_4(\mathbf{r})$ . The coherent state now becomes

$$\begin{aligned} |\psi\rangle &= \prod_{r=\text{even}} e^{(\eta_{00}(r)D^\dagger(\mathbf{r}) + \eta_{10}(r)\pi_z^\dagger(\mathbf{r}) - \text{h. c.})} |0^*\rangle \\ &\equiv \mathcal{T} |0^*\rangle, \end{aligned}$$

where  $\mathcal{T}$  is a direct product of the  $\mathcal{T}(r)$ ,

$$\mathcal{T} = \prod_{r=\text{even}} \mathcal{T}(\mathbf{r}) = \prod_{r=\text{even}} \begin{bmatrix} \mathbf{Y}_1(\mathbf{r}) & \mathbf{X}(\mathbf{r}) \\ -\mathbf{X}^\dagger(\mathbf{r}) & \mathbf{Y}_2(\mathbf{r}) \end{bmatrix},$$

with

$$\begin{aligned} \mathbf{X}(\mathbf{r}) &\equiv \begin{bmatrix} 0 & v_{r+} \\ -v_{r-} & 0 \end{bmatrix} \\ \mathbf{Y}_1(\mathbf{r}) &\equiv \begin{bmatrix} u_{r+} & 0 \\ 0 & u_{r-} \end{bmatrix} \\ \mathbf{Y}_2(\mathbf{r}) &\equiv \begin{bmatrix} u_{r-} & 0 \\ 0 & u_{r+} \end{bmatrix}. \end{aligned}$$

The variational Hamiltonian is

$$\begin{aligned} H' &= H - \lambda \hat{n} \\ &= \sum_{r=\text{even}} (\varepsilon_r - \lambda) \hat{n}_r \\ &\quad - \left( G_0 D^\dagger D + G_1 \vec{\pi}^\dagger \cdot \vec{\pi} + \chi \vec{Q} \cdot \vec{Q} + \kappa \vec{S} \cdot \vec{S} \right). \end{aligned}$$

Taking expectation values of operators as in Eqs. (A9) and (A10) permits the expectation value of  $H'$  to be determined. However, to consider the temperature dependence, one should replace the quasiparticle vacuum state  $|\psi\rangle$  by the state  $|\psi(T)\rangle$  in which quasiparticles are thermally excited. The expectation values of  $a_{rj}^\dagger a_{rj}$  and  $a_{\bar{r}i}^\dagger a_{\bar{r}j}$  in (A5) are no longer zero when  $i = j$ . Therefore, instead of (A7), the formula to evaluate expectation values for a one-body operator becomes

$$\begin{aligned} \langle \hat{O} \rangle &= \langle \psi(T) | \hat{O} | \psi(T) \rangle \\ &= \sum_{r=\text{even}} \left\{ \mathcal{O}_{11}^{(22)}(r) + \mathcal{O}_{22}^{(22)}(r) \right. \\ &\quad + [\mathcal{O}_{11}^{(11)}(r) \tilde{n}_{r\uparrow}(T) - \mathcal{O}_{22}^{(22)}(r) \tilde{n}_{\bar{r}\downarrow}(T)] \\ &\quad \left. + [\mathcal{O}_{22}^{(11)}(r) \tilde{n}_{r\downarrow}(T) - \mathcal{O}_{11}^{(22)}(r) \tilde{n}_{\bar{r}\uparrow}(T)] \right\}. \quad (\text{B2}) \end{aligned}$$

In Eq. (B2), we have supposed that at temperature  $T$ ,  $\tilde{n}_{ri}(T)$  and  $\tilde{n}_{\bar{r}i}(T)$  are respectively the numbers of quasiparticles at  $r$  and  $\bar{r}$  with spin  $i$ ,

$$\begin{aligned} \langle \psi(T) | a_{ri}^\dagger a_{ri} | \psi(T) \rangle &= \tilde{n}_{ri}(T) \\ \langle \psi(T) | a_{\bar{r}i}^\dagger a_{\bar{r}i} | \psi(T) \rangle &= \tilde{n}_{\bar{r}i}(T). \end{aligned}$$

It can be shown that for all the  $SU(4)$  generators except spin  $\vec{S}$ ,

$$\mathcal{O}_{11}^{(11)}(r) = -\mathcal{O}_{22}^{(22)}(r) \quad \mathcal{O}_{22}^{(11)}(r) = -\mathcal{O}_{11}^{(22)}(r),$$

and therefore

$$\begin{aligned} \langle \hat{O} \rangle &= \langle \psi | \hat{O} | \psi \rangle \\ &= \sum_{r=\text{even}} \left\{ \mathcal{O}_{11}^{(22)}(r) [1 - \tilde{n}_{r-}(T)] \right. \\ &\quad \left. + \mathcal{O}_{22}^{(22)}(r) [1 - \tilde{n}_{r+}(T)] \right\}, \quad (\text{B3}) \end{aligned}$$

where

$$\tilde{n}_{r+} \equiv a_{r\uparrow}^\dagger a_{r\uparrow} + a_{\bar{r}\downarrow}^\dagger a_{\bar{r}\downarrow}, \quad \tilde{n}_{r-} \equiv a_{\bar{r}\downarrow}^\dagger a_{\bar{r}\downarrow} + a_{r\uparrow}^\dagger a_{r\uparrow}. \quad (\text{B4})$$

As for Eq. (A9), one can use Eq. (B3) to obtain the one-body terms

$$\begin{aligned} \langle D^\dagger(r) \rangle &= \langle D(r) \rangle \\ &= -[P_{r+}(T)u_{r+}v_{r+} \\ &\quad + P_{r-}(T)u_{r-}v_{r-}] \quad (\text{B5a}) \end{aligned}$$

$$\begin{aligned} \langle \pi_z^\dagger(r) \rangle &= \langle \pi_z(r) \rangle \\ &= -[P_{r+}(T)u_{r+}v_{r+} \\ &\quad - P_{r-}(T)u_{r-}v_{r-}] \quad (\text{B5b}) \end{aligned}$$

$$\begin{aligned} \langle \vec{Q}(r) \rangle &= \langle Q_z(r) \rangle \\ &= \frac{1}{2} [P_{r+}(T)(2v_{r+}^2 - 1) \\ &\quad - P_{r-}(T)(2v_{r-}^2 - 1)] \quad (\text{B5c}) \end{aligned}$$

$$\begin{aligned} \langle M(r) \rangle &= \frac{1}{2} n_r - 1 \\ &= \frac{1}{2} [P_{r+}(T)(2v_{r+}^2 - 1) \\ &\quad + P_{r-}(T)(2v_{r-}^2 - 1)], \quad (\text{B5d}) \end{aligned}$$

where

$$P_{r\pm}(T) = 1 - \tilde{n}_{r\pm}(T).$$

As in Eqs. (A9),  $\langle \pi_x \rangle$ ,  $\langle \pi_y \rangle$ ,  $\langle \vec{Q}_x \rangle$ ,  $\langle \vec{Q}_y \rangle$ , and  $\langle \vec{S} \rangle$  are all zero. Note that for spin this is true only when the quasiparticles result from thermal excitations. This is because from (B2) one can show that

$$\begin{aligned} \langle \vec{S}(r) \rangle &= \langle S_z(r) \rangle \\ &= \frac{1}{2} \{ (\tilde{n}_{r\uparrow} - \tilde{n}_{\bar{r}\downarrow}) - (\tilde{n}_{r\downarrow} - \tilde{n}_{\bar{r}\uparrow}) \}, \end{aligned}$$

which is generally nonzero. Only when the quasiparticles are due to thermal excitations, as we will show later,

we do have  $\tilde{n}_{r\uparrow} = \tilde{n}_{r\downarrow}$  and  $\tilde{n}_{r\downarrow} = \tilde{n}_{r\uparrow}$ , which leads to  $\langle S_z(r) \rangle = 0$ .

Applying the large- $\Omega$  approximation (ignoring the second term in Eq. (A8) when  $\Omega \rightarrow \infty$ ), one obtains the two-body terms

$$\begin{aligned} \langle D^\dagger D \rangle &= \langle D \rangle^2 \\ &= \left\{ \sum_{r=\text{even}} [P_{r+}(T)u_{r+}v_{r+} \right. \\ &\quad \left. + P_{r-}(T)u_{r-}v_{r-}] \right\}^2 \end{aligned} \quad (\text{B6a})$$

$$\begin{aligned} \langle \vec{\pi}^\dagger \cdot \vec{\pi} \rangle &= \langle \pi_z \rangle^2 \\ &= \left\{ \sum_{r=\text{even}} [P_{r+}(T)u_{r+}v_{r+} \right. \\ &\quad \left. - P_{r-}(T)u_{r-}v_{r-}] \right\}^2 \end{aligned} \quad (\text{B6b})$$

$$\begin{aligned} \langle \vec{Q} \cdot \vec{Q} \rangle &= \langle Q_z \rangle^2 \\ &= \frac{1}{4} \left\{ \sum_{r=\text{even}} [P_{r+}(T)(v_{r+}^2 - u_{r+}^2) \right. \\ &\quad \left. - P_{r-}(T)(v_{r-}^2 - u_{r-}^2)] \right\}^2 \end{aligned} \quad (\text{B6c})$$

$$\begin{aligned} \langle M \rangle &= -\frac{1}{2}x\Omega \\ &= \frac{1}{2} \sum_{r=\text{even}} [P_{r+}(T)(v_{r+}^2 - u_{r+}^2) \\ &\quad + P_{r-}(T)(v_{r-}^2 - u_{r-}^2)]. \end{aligned} \quad (\text{B6d})$$

The next operations are similar to those of section III.C. By introducing the energy gaps

$$\Delta_d = |G_0 \langle D \rangle| \quad \Delta_\pi = |G_0 \langle \pi_z \rangle| \quad \Delta_q = |\chi \langle \vec{Q}_z \rangle|,$$

defining  $\varepsilon_{r\pm}$  and  $\Delta_\pm$ , and utilizing (B5) to construct  $\langle H' \rangle$  and perform the variation calculation  $\delta \langle H' \rangle = 0$ , one obtains

$$2u_{r\pm}v_{r\pm}(\varepsilon_{r\pm} - \lambda) - \Delta_\pm(u_{r\pm}^2 - v_{r\pm}^2) = 0. \quad (\text{B7})$$

Solving this equation gives

$$u_{r\pm}^2 = \frac{1}{2} \left[ 1 + \frac{\varepsilon_{r\pm} - \lambda}{e_{r\pm}} \right] \quad (\text{B8a})$$

$$v_{r\pm}^2 = \frac{1}{2} \left[ 1 - \frac{\varepsilon_{r\pm} - \lambda}{e_{r\pm}} \right] \quad (\text{B8b})$$

with quasiparticle energies defined as

$$e_{r\pm} = \sqrt{(\varepsilon_{r\pm} - \lambda)^2 + \Delta_\pm^2}. \quad (\text{B9})$$

Inserting Eqs. (B8) into Eqs. (B5) and (B6), one finds the gap equations:

$$\begin{aligned} \Delta_d &= \frac{G_0}{2} \sum_{r=\text{even}} \left[ \frac{P_{r+}(T)}{e_{r+}} \Delta_+ \right. \\ &\quad \left. + \frac{P_{r-}(T)}{e_{r-}} \Delta_- \right] \end{aligned} \quad (\text{B10a})$$

$$\begin{aligned} \Delta_\pi &= \frac{G_1}{2} \sum_{r=\text{even}} \left[ \frac{P_{r+}(T)}{e_{r+}} \Delta_+ \right. \\ &\quad \left. - \frac{P_{r-}(T)}{e_{r-}} \Delta_- \right] \end{aligned} \quad (\text{B10b})$$

$$\begin{aligned} \Delta_q &= \frac{\chi}{2} \sum_{r=\text{even}} \left[ \frac{P_{r+}(T)}{e_{r+}} (\lambda - \varepsilon_{r+}) \right. \\ &\quad \left. - \frac{P_{r-}(T)}{e_{r-}} (\lambda - \varepsilon_{r-}) \right] \end{aligned} \quad (\text{B10c})$$

$$\begin{aligned} -2x &= \frac{2}{\Omega} \sum_{r=\text{even}} \left[ \frac{P_{r+}(T)}{e_{r+}} (\lambda - \varepsilon_{r+}) \right. \\ &\quad \left. + \frac{P_{r-}(T)}{e_{r-}} (\lambda - \varepsilon_{r-}) \right], \end{aligned} \quad (\text{B10d})$$

The energy of the system is then obtained as

$$\begin{aligned} E(T) &= \langle H' \rangle + n\lambda \\ &= \sum_r n_r \varepsilon_r - \left[ \frac{\Delta_d^2}{G_0} + \frac{\Delta_\pi^2}{G_1} + \frac{\Delta_q^2}{\chi} \right]. \end{aligned}$$

Utilizing Eqs. (B8)–(B10), it can be shown that

$$\begin{aligned} &-2 \left[ \frac{\Delta_d^2}{G_0} + \frac{\Delta_\pi^2}{G_1} + \frac{\Delta_q^2}{\chi} \right]_{T=0} + \sum_{r=\text{even}} (\varepsilon_r - \lambda) n_r \\ &= \sum_{r=\text{even}} [2(\varepsilon_r - \lambda) - P_{r+}(T)e_{r+} - P_{r-}(T)e_{r-}]. \end{aligned}$$

This relation can be used to rewrite the energy as a sum of the quasiparticle vacuum energy and the quasiparticle excitation energy

$$E(T) = E_0(T) + \sum_{r=\text{even}} \{ \tilde{n}_{r+}(T) e_{r+} + \tilde{n}_{r-}(T) e_{r-} \}. \quad (\text{B11})$$

In the above equation, the quasiparticle vacuum energy is

$$\begin{aligned} E_0(T) &= \sum_{r=\text{even}} (2\varepsilon_r - e_{r+} - e_{r-}) - (\Omega - n)\lambda \\ &\quad + \left[ \frac{\Delta_d^2}{G_0} + \frac{\Delta_\pi^2}{G_1} + \frac{\Delta_q^2}{\chi} \right]_{T=0}, \end{aligned} \quad (\text{B12})$$

which is determined by solving the gap equations (B10) at  $T = 0$ , while the quasiparticle number operators are assumed to be

$$\tilde{n}_{r\pm}(T) = \frac{2}{1 + \exp\left(\frac{e_{r\pm}}{k_B T}\right)},$$

since they are associated with thermal fluctuations, and thus

$$P_{r\pm}(T) = 1 - \tilde{n}_{r\pm}(T) = \tanh\left(\frac{e_{r\pm}}{2k_B T}\right).$$

Note that, according to the definition (B4),

$$\begin{aligned}\tilde{n}_{r+}(T) &= \tilde{n}_{r\uparrow}(T) + \tilde{n}_{\bar{r}\downarrow}(T) \\ \tilde{n}_{r-}(T) &= \tilde{n}_{r\downarrow}(T) + \tilde{n}_{\bar{r}\uparrow}(T).\end{aligned}$$

Therefore, Eq. (B11) implies that the quasiparticle states  $|r\uparrow\rangle$  and  $|\bar{r}\downarrow\rangle$  are degenerate with excitation energy  $e_{r+}$ , while the states  $|r\downarrow\rangle$  and  $|\bar{r}\uparrow\rangle$  are degenerate with excitation energy  $e_{r-}$ . Thus, as we have mentioned before,

$$\begin{aligned}\tilde{n}_{r\uparrow}(T) &= \tilde{n}_{\bar{r}\downarrow}(T) = \frac{1}{1 + \exp\left(\frac{e_{r+}}{k_B T}\right)} \\ \tilde{n}_{r\downarrow}(T) &= \tilde{n}_{\bar{r}\uparrow}(T) = \frac{1}{1 + \exp\left(\frac{e_{r-}}{k_B T}\right)}.\end{aligned}$$

The physical meaning of  $\Delta_q$  can now be better understood. From the expression for the quasiparticle energies  $e_{r\pm}$ , one sees that the original four-fold degeneracy of the single-particle energy level  $\varepsilon_r$  has been split into a two-fold degeneracy because of the  $\vec{Q} \cdot \vec{Q}$  interaction:

$$\begin{aligned}\varepsilon_{r+} &= \varepsilon_r - \Delta_q & (|r\uparrow\rangle \text{ and } |\bar{r}\downarrow\rangle) \\ \varepsilon_{r-} &= \varepsilon_r + \Delta_q & (|r\downarrow\rangle \text{ and } |\bar{r}\uparrow\rangle).\end{aligned}$$

The energy difference  $2\Delta_q$  is just the energy required to flip the spin of an electron from  $|r\uparrow\rangle$  to  $|r\downarrow\rangle$  or from  $|\bar{r}\uparrow\rangle$  to  $|\bar{r}\downarrow\rangle$ , and *vice versa*.

The above results can also be obtained through a mean field approximation. Note that any two-body operator of the form  $\hat{O}_A \hat{O}_B$  can always be written as

$$\begin{aligned}\hat{O}_A \hat{O}_B &= [(\hat{O}_A) + (\hat{O}_A - \langle \hat{O}_A \rangle)] \\ &\quad \times [(\hat{O}_B) + (\hat{O}_B - \langle \hat{O}_B \rangle)] \\ &= \langle \hat{O}_A \rangle \langle \hat{O}_B \rangle + \hat{O}_A (\hat{O}_B - \langle \hat{O}_B \rangle) \\ &\quad + (\hat{O}_A - \langle \hat{O}_A \rangle) \hat{O}_B \\ &\quad + (\hat{O}_A - \langle \hat{O}_A \rangle) (\hat{O}_B - \langle \hat{O}_B \rangle).\end{aligned}$$

Suppose that the last term of the preceding equation can be ignored, implying that the physical effects of  $(\hat{O}_A - \langle \hat{O}_A \rangle)$  and  $(\hat{O}_B - \langle \hat{O}_B \rangle)$  are small. Then the two-body operator reduces to an one-body operator:

$$\hat{O}_A \hat{O}_B = -\langle \hat{O}_A \rangle \langle \hat{O}_B \rangle + \hat{O}_A \langle \hat{O}_B \rangle + \langle \hat{O}_A \rangle \hat{O}_B.$$

Applying this equation to the Hamiltonian (B1),

$$H = H_0 + \sum_{r=\text{even}} h(r),$$

where  $H_0$  is a c-number

$$\begin{aligned}H_0 &= \sum_{r=\text{even}} 2\varepsilon_r - (\Omega - n)\lambda \\ &\quad + \left[ \frac{\Delta_d^2}{G_0} + \frac{\Delta_\pi^2}{G_1} + \frac{\Delta_q^2}{\chi} \right],\end{aligned}\quad (\text{B13})$$

the subscript 0 denotes a ground state expectation value, we have made the replacements

$$-G_0 \langle D \rangle \rightarrow \Delta_d, \quad -G_1 \langle \pi_z \rangle \rightarrow \Delta_\pi, \quad \chi \langle Q_z \rangle \rightarrow \Delta_q,$$

and the second term in  $H$  defines a mean field

$$\begin{aligned}h(r) &= 2(\varepsilon_r - \lambda)M(r) + \{\Delta_d[D^\dagger(r) + D(r)] \\ &\quad + \Delta_\pi[\pi_z^\dagger(r) + \pi_z(r)] - 2\Delta_q Q_z\}.\end{aligned}\quad (\text{B14})$$

Now we implement a quasiparticle transformation on  $H$ ,

$$\mathcal{H} \equiv \mathcal{T} H \mathcal{T}^{-1} = H_0 + \sum_{r=\text{even}} \tilde{h}(r),$$

where

$$\tilde{h}(r) \equiv \mathcal{T} h(r) \mathcal{T}^{-1} = \begin{pmatrix} \tilde{h}^{(11)}(r) & \tilde{h}^{(12)}(r) \\ \tilde{h}^{(21)}(r) & \tilde{h}^{(22)}(r) \end{pmatrix}$$

and

$$\begin{aligned}\tilde{h}^{(11)}(r) &= \begin{pmatrix} e_{r+} & 0 \\ 0 & e_{r-} \end{pmatrix} \\ \tilde{h}^{(22)}(r) &= \begin{pmatrix} -e_{r-} & 0 \\ 0 & -e_{r+} \end{pmatrix} \\ \tilde{h}^{(12)}(r) &= \tilde{h}^{(21)}(r)^\dagger = \begin{pmatrix} 0 & \mathcal{O}_+ \\ -\mathcal{O}_- & 0 \end{pmatrix},\end{aligned}$$

with

$$\begin{aligned}\mathcal{O}_\pm &= \Delta_\pm (u_{r\pm}^2 - v_{r\pm}^2) \\ &\quad - (\varepsilon_{r\pm} - \lambda) 2u_{r\pm} v_{r\pm},\end{aligned}\quad (\text{B15})$$

$$\begin{aligned}e_{r\pm} &= (\varepsilon_{r\pm} - \lambda) (u_{r\pm}^2 - v_{r\pm}^2) \\ &\quad + \Delta_\pm 2u_{r\pm} v_{r\pm}.\end{aligned}\quad (\text{B16})$$

The condition for the Hamiltonian  $\mathcal{H}$  to be diagonal is that Eq. (B15) be zero, which is equivalent to Eq. (B7). The solutions of  $u_{r\pm}$  and  $v_{r\pm}$  are the same as those in Eqs. (B8). Inserting these  $u$ 's and  $v$ 's into Eq. (B16), one can check that the  $e_{r\pm}$  appearing in (B10) are indeed the quasiparticle energies defined in (B9).

In the expression for an operator [see Eq. (A1)],  $\tilde{h}(r)$  can be written as

$$\begin{aligned}\tilde{h}(r) &= e_{r+} a_{r\uparrow}^\dagger a_{r\uparrow} + e_{r-} a_{r\downarrow}^\dagger a_{r\downarrow} \\ &\quad - e_{r-} a_{\bar{r}\uparrow}^\dagger a_{\bar{r}\uparrow} - e_{r+} a_{\bar{r}\downarrow}^\dagger a_{\bar{r}\downarrow} \\ &= -(e_{r+} + e_{r-}) + (\tilde{n}_{r+} e_{r+} + \tilde{n}_{r-} e_{r-}).\end{aligned}$$

Since

$$H_0 - \sum_r (e_{r+} + e_{r-}) = E_0$$

[see (B12) and (B13)], the Hamiltonian may be written as

$$\mathcal{H} = E_0 + \sum_{r=\text{even}} [\tilde{n}_{r+} e_{r+} + \tilde{n}_{r-} e_{r-}], \quad (\text{B17})$$

which is Eq. (B11). If we ignore single-particle energy splitting,  $u$  and  $v$  have no  $r$  dependence, meaning that  $\sum_r = \Omega/2$ , and in this case all results reduce to those discussed in Section III.

From the preceding discussion it becomes clear that the SU(4) coherent state is in fact a mean field solution of the SU(4) Hamiltonian. The SU(4) coherent state may thus be viewed as a generalization of the BCS theory, and the process to derive it can be characterized as a Hartree–Fock–Bogoliubov (HFB) transformation that implements a (non-abelian) symmetry constraint on the variational wavefunction. It is a generalized BCS theory because the system contains two kinds of quasiparticles instead of one. In addition, the  $\vec{Q} \cdot \vec{Q}$  interaction splits the single-particle energy levels into two sets,

$$\varepsilon_{r\pm} = \varepsilon_r \mp \Delta_q.$$

These new features are primarily responsible for the differences between high- $T_c$  superconductivity and conventional superconductivity described by the ordinary BCS theory.

### APPENDIX C: GENERAL SOLUTIONS OF THE GAP EQUATIONS

The temperature-dependent gap equations are coupled algebraic equations. In this section we present one way to solve these equations. First, we rewrite Eqs. (18a) and (18b) in the form

$$\begin{aligned} (\omega_0 - w_+) \Delta_d + (\omega_1 - w_+) \Delta_\pi &= 0 \\ (\omega_0 - w_-) \Delta_d - (\omega_1 - w_-) \Delta_\pi &= 0 \end{aligned}$$

with

$$\omega_0 = \frac{2}{G_0 \Omega} \quad \omega_1 = \frac{2}{G_1 \Omega}.$$

The condition for these coupled equations to have solutions is

$$(\omega_0 - w_+) (\omega_1 - w_-) + (\omega_1 - w_+) (\omega_0 - w_-) = 0.$$

One then obtains

$$w_\pm = \bar{\omega} \frac{w_\mp - \tilde{\omega}}{w_\mp - \bar{\omega}} \quad \bar{\omega} = \frac{\omega_0 + \omega_1}{2} \quad \tilde{\omega} = \frac{\omega_0 \omega_1}{\bar{\omega}} \quad (\text{C1})$$

and

$$\begin{aligned} \Delta_\pi &= \left( \frac{w_- - \omega_0}{w_- - \omega_1} \right) \Delta_d \\ \Delta_\pi &= - \left( \frac{w_+ - \omega_0}{w_+ - \omega_1} \right) \Delta_d. \end{aligned} \quad (\text{C2})$$

By using Eqs. (18) and the new equations (C1) and (C2), a formal solution in terms of  $w_\pm$  can be expressed as

$$\Delta_d = G_0 \Omega \sqrt{\frac{(I - x^2)/4 - (\Delta_q/\chi\Omega)^2}{1 + \left( \frac{1 - w_+/\omega_0}{1 - w_+/\omega_1} \right)^2}} \quad (\text{C3a})$$

$$\Delta_\pi = G_1 \Omega \sqrt{\frac{(I - x^2)/4 - (\Delta_q/\chi\Omega)^2}{1 + \left( \frac{1 - w_+/\omega_1}{1 - w_+/\omega_0} \right)^2}} \quad (\text{C3b})$$

$$\Delta_q = \frac{\chi}{2} \Omega \left| \frac{x(w_+ - w_-)}{\chi\Omega w_+ w_- - (w_+ + w_-)} \right| \quad (\text{C3c})$$

$$\lambda' = -\frac{x}{2} \left| \frac{\chi\Omega(w_+ + w_-) - 4}{\chi\Omega w_+ w_- - (w_+ + w_-)} \right|, \quad (\text{C3d})$$

where we have made use of the SU(4) invariant [see Eq. (7)]

$$\langle \mathcal{E}_{\text{SU4}} \rangle = \frac{\Omega^2}{4} (I - x^2) \quad I = (1 - u)^2, \quad (\text{C4})$$

and  $u$  is the unpaired number density.

Eqs. (C3) represent a formal solution only since  $w_\pm$  must be determined from Eq. (19) in a self-consistent manner. This can be done by combining Eqs. (19), (C1), and (C3). It turns out that  $w_+$  and  $w_-$  satisfy the same equation. Adopting the notation  $w_\pm \equiv w$ , we have

$$y^2 = \frac{\omega_0 \omega_1 [w^2(\omega_0 + \omega_1 - 2\omega_q) - 2w\omega_0\omega_1 + 2\omega_0\omega_1\omega_q]^2}{w^2[w(\omega_0 + \omega_1) - 2\omega_0\omega_1]^2(\omega_0 - 2\omega_q)(\omega_1 - 2\omega_q)} \quad (\text{C5})$$

with

$$\omega_q = \frac{1}{\chi\Omega}.$$

and for the left side of Eq. (C5)

$$y \equiv y_\pm = \frac{x}{\sqrt{I[1 \pm \delta_\pm \Gamma(y)]}}, \quad (\text{C6})$$

with

$$\begin{aligned} \delta_\pm &= 1 - \frac{P_\pm(T)^2}{I} \\ &= 1 - \frac{\tanh^2(e_\pm/2k_B T)}{I} \end{aligned} \quad (\text{C7})$$

$$\Gamma(y) = \left| 1 + \frac{w^2(\omega_0 - \omega_1)^2}{2\omega_0\omega_1(\omega - \omega_0)(\omega - \omega_1)} \right|. \quad (\text{C8})$$

Eqs. (C3) now become

$$\Delta_d = \frac{|(\omega_1 - w)|\sqrt{1 - x^2 - (2\omega_q\Delta_q)^2}}{\sqrt{\omega_0^2(w - \omega_1)^2 + \omega_1^2(w - \omega_0)^2}} \quad (\text{C9a})$$

$$\Delta_\pi = \frac{|(w - \omega_0)|\sqrt{1 - x^2 - (2\omega_q\Delta_q)^2}}{\sqrt{\omega_0^2(w - \omega_1)^2 + \omega_1^2(w - \omega_0)^2}} \quad (\text{C9b})$$

$$\Delta_q = \frac{x}{2} \left| \frac{(w - \omega_0)(w - \omega_1)}{w^2(\bar{\omega} - \omega_q) - w\omega_0\omega + \omega_q\omega_0\omega_1} \right| \quad (\text{C9c})$$

$$\lambda' = -\frac{x}{2} \left| \frac{(w^2) - 4\omega_q w + (4\omega_q \bar{\omega} - \omega_0\omega_1)}{w^2(\bar{\omega} - \omega_q) - w\omega_0\omega + \omega_q\omega_0\omega_1} \right| \quad (\text{C9d})$$

By introducing the variables

$$q_0 = 1 - \frac{2\omega_q}{\omega_0} \quad q_1 = 1 - \frac{2\omega_q}{\omega_1} \quad \bar{q} = 1 - \frac{\omega_q}{\tilde{\omega}}$$

and

$$x_q^2 = \frac{\chi - G_0}{\chi - G_1} = \frac{q_0}{q_1}, \quad (\text{C10})$$

Eq. (C5) can be greatly simplified:

$$\frac{y}{x_q} = \pm \frac{\bar{q}w^2 - \tilde{\omega}w + \tilde{\omega}}{q_0w(w - \tilde{\omega})}. \quad (\text{C11})$$

The signs “ $\pm$ ” are for hole doping ( $x, y > 0$ ) and electron doping ( $x, y < 0$ ), respectively. Obviously, this means that the solution has particle-hole symmetry:  $w$  depends only on the absolute value of  $y$  (or  $x$ ). For this reason, we shall regard  $y$  as the absolute value  $|y|$  and ignore the  $\pm$  sign in the following discussions. Solving the quadratic equation (C11) gives

$$w = \frac{2}{\epsilon(y)}, \quad (\text{C12})$$

$$\epsilon(y) = \left( \chi - (\chi - G_0) \frac{y}{x_q} \right) - \eta (\chi - G_1) \sqrt{x_q(x_q - y)(1 - x_q y)}, \quad (\text{C13})$$

where  $\eta = \pm 1$ . Eqs. (C12) and (C13) determine the value of  $w$  and thus of  $w_{\pm}$ . Since  $w_+ \geq w_-$ , in Eq. (C13),  $\eta = +1$  for  $w_+$  and  $\eta = -1$  for  $w_-$ .

Inserting Eq. (C13) into Eqs. (C8) and (C9) gives

$$\Gamma(y) = \left| 1 + \frac{(G_0 - G_1)^2}{2[G_0 - \epsilon(y)][G_1 - \epsilon(y)]} \right| \quad (\text{C14})$$

$$\Delta_q = \frac{\chi}{2} \Omega q(y) \quad \Delta_{\pi} = \frac{G_1}{2} \Omega T(y) \quad (\text{C15})$$

$$\Delta_d = \frac{G_0}{2} \Omega S(y) \quad \lambda' = -\frac{\gamma(y)}{2} \Omega x$$

with

$$q(y) = \frac{[\epsilon(y) - G_0][\epsilon(y) - G_1] x}{\epsilon(y)^2 - [2\epsilon(y) - G_0 - G_1]\chi - G_0 G_1} \quad (\text{C16a})$$

$$T(x) = [\epsilon(y) - G_1] \sqrt{\frac{I - x^2 - q(y)^2}{[G_0 - \epsilon(y)]^2 + [G_1 - \epsilon(y)]^2}} \quad (\text{C16b})$$

$$S(y) = [G_0 - \epsilon(y)] \sqrt{\frac{I - x^2 - q(y)^2}{[G_0 - \epsilon(y)]^2 + [G_1 - \epsilon(y)]^2}} \quad (\text{C16c})$$

$$\gamma(x) = \frac{\epsilon(y)^2(G_0 + G_1 - \chi) + G_0 G_1[\chi - 2\epsilon(y)]}{\epsilon(y)^2 - [2\epsilon(y) - G_0 - G_1]\chi - G_0 G_1}. \quad (\text{C16d})$$

Eqs. (C16) can be further simplified by using Eq. (C10) and recognizing that

$$\begin{aligned} \epsilon(y) - G_0 &= -(\chi - G_1) (\eta ab - a^2) \\ \epsilon(y) - G_1 &= (\chi - G_1) (b^2 - \eta ab) \\ \epsilon(y) - \chi &= -(\chi - G_1) (x_q y + \eta ab) \end{aligned}$$

where

$$a \equiv \sqrt{x_q(x_q - y)} \quad b \equiv \sqrt{1 - x_q y}. \quad (\text{C17})$$

In terms of  $a$  and  $b$ , Eqs. (C14) and (C16) can be rewritten as

$$\begin{aligned} \Gamma(y) &= \frac{a^2 + b^2}{2ab} \\ q(y) &= \frac{abx}{x_q y} \\ T(y) &= a \sqrt{\frac{(I - x^2) x_q^2 - a^2 b^2}{(a^2 + b^2) x_q^2}} \\ S(y) &= b \sqrt{\frac{(I - x^2) x_q^2 - a^2 b^2}{(a^2 + b^2) x_q^2}} \\ \gamma(y) &= (\chi - G_1) \frac{a^2 b^2 - (x_q y)^2}{x_q y} + \chi. \end{aligned}$$

Using Eq. (C17) to convert  $a$  and  $b$  back to  $y$  yields

$$\begin{aligned} \Gamma(y) &= \frac{(1 - y^2) + (x_q - y)^2}{2\sqrt{x_q(x_q - y)}(1 - x_q y)} \\ q(y) &= \sqrt{(x_q - y)(x_q^{-1} - y)} \frac{x}{y} \\ T(y) &= \sqrt{x(x_q - y)} g(y) \\ S(y) &= \sqrt{x(x_q^{-1} - y)} g(y) \\ \gamma(y) &= (\chi - G_1) \frac{x_q(1 - x_q y)}{y} + G_1 \\ g(y) &= \sqrt{\frac{x}{y} + \frac{x_q(Iy^2 - x^2)}{xy^2(1 - 2x_q y + x_q^2)}}. \end{aligned}$$

Inserting the above results into Eqs. (C15) and taking into account the definition of  $x_q$  in Eq. (C10) gives Eqs. (30) in Sect. V.A.

$$\begin{aligned} \Delta_q &= \frac{\chi \Omega}{2} \sqrt{(x_q^{-1} - y)(x_q - y)} \frac{x}{y} \\ \Delta_d &= \frac{G_0 \Omega}{2} \sqrt{x(x_q^{-1} - y)} g(y) \\ \Delta_{\pi} &= \frac{G_1 \Omega}{2} \sqrt{x(x_q - y)} g(y) \\ \lambda' &= \frac{(G_1 - \chi) \Omega}{2} x_q \left( \frac{x}{y} - x_q x \right) - \frac{G_1 \Omega}{2} x. \end{aligned}$$

For  $T = 0$ , from Eq. (C6), one obtains immediately

$$y = y_{\pm} = x$$

because  $\delta_{\pm} \rightarrow 0$ . We thus have the results of Eqs. (24) discussed in Sect. IV.A. For  $T > 0$ , however, the self-consistency condition  $y = y_+ = y_-$  must be satisfied, which requires that

$$\sqrt{I[1 + \delta_+ \Gamma(y)]} = \sqrt{I[1 - \delta_- \Gamma(y)]}$$

and thus that  $\delta_+ + \delta_- = 0$ . According to Eq. (C7), this can be fulfilled only if

$$I = \frac{\tanh^2(e_+/2k_B T) + \tanh^2(e_-/2k_B T)}{2},$$

which implies the existence of unpaired particles. The density of unpaired particles can be deduced from Eq. (C4):

$$(1 - u) = \sqrt{\frac{\tanh^2\left(\frac{e_+}{2k_B T}\right) + \tanh^2\left(\frac{e_-}{2k_B T}\right)}{2}}.$$

This completes the derivation. Methods to obtain the actual gap values for given  $x$  and  $T$  from the above equations have been discussed extensively in Section V.

- 
- [1] T. Timusk and B. Statt, Rep. Prog. Phys. **62**, 61 (1999).  
[2] A. Damascelli, Z. Hussain, and Z.-X. Shen, Rev. Mod. Phys. **75**, 473 (2003).  
[3] P. W. Anderson, Physica **C 341 - 348**, 9 (2000); D. Pines, Physica **C 341 - 348**, 59 (2000); R. B. Laughlin and D. Pines, PNAS **97**, 28 (2000).  
[4] F. Iachello and A. Arima, *The Interacting Boson Model* (Cambridge University Press, Cambridge, 1987).  
[5] C.-L. Wu, D. H. Feng and M. W. Guidry, Adv. in Nucl. Phys. **21**, 227 (1994).  
[6] F. Iachello and R. D. Levine, *Algebraic Theory of Molecules* (Oxford University Press, New York, 1995).  
[7] F. Iachello and P. Truini, Ann. Phys. (N.Y.) **276**, 120 (1999).  
[8] R. Bijker, F. Iachello, and A. Leviatan, Ann. Phys. (N.Y.) **236**, 69 (1994).  
[9] M. Guidry, L.-A. Wu, Y. Sun, and C.-L. Wu, Phys. Rev. **B 63**, 134516 (2001).  
[10] L.-A. Wu, M. Guidry, Y. Sun, and C.-L. Wu, Phys. Rev. **B 67**, 014515 (2003).  
[11] M. Guidry, Y. Sun and C.-L. Wu, Phys. Rev. **B 70**, 184501 (2004).  
[12] R. S. Markiewicz and M. T. Vaughn, J. Phys. Chem. Sol. **59**, 1737 (1998); J. L. Birman and M. Weger, Phys. Rev. **B 64**, 174503 (2001); J. Dukelsky, S. Pittel, and G. Sierra, Rev. Mod. Phys. **76**, 643 (2004); T. Kuzmenko, K. Kikoin, and Y. Avishai, Phys. Rev. **B 69**, 195109 (2004).  
[13] S.-C. Zhang, Science **275**, 1089 (1997).  
[14] The particle-hole symmetry intrinsic to the SU(4) model does not mean that hole-doped and electron-doped cuprates are expected to behave in the same manner. Although the states of the model are particle-hole symmetric, the interactions entering the effective Hamiltonian would not be expected to be the same for hole-doped and particle-doped compounds. We shall show in future publications that electron-doped cuprates are predicted to behave very differently than hole-doped cuprates in the SU(4) model. One consequence is a prediction that it is difficult to obtain superconductivity in electron-doped cuprates.  
[15] D. J. Scalapino, Phys. Rep. **250**, 329 (1995).  
[16] E. Demler and S.-C. Zhang, Phys. Rev. Lett. **75**, 4126 (1995).  
[17] W.-M. Zhang, D. H. Feng and R. Gilmore, Rev. Mod. Phys. **62**, 867 (1990).  
[18] Generally, the term  $\eta_{10}q_{12}^\dagger$  in Eq. (10) should be  $\vec{\eta}_1 \cdot \vec{\pi}^\dagger$ , and the parameters could be complex as well. Thus the most general SU(4) coherent state depends on eight real variables. The reduction of the coherent state parameters to only two in Eq. (10) follows from requiring time reversal symmetry and assuming conservation of spin projection  $S_z$  for the wavefunction.  
[19] W.-M. Zhang, C.-L. Wu, D. H. Feng, J. N. Ginocchio, and M. W. Guidry, Phys. Rev. **C38**, 1475 (1988); W.-M. Zhang, D. H. Feng, C.-L. Wu, H. Wu, and J. N. Ginocchio, Nucl. Phys. **A505**, 7 (1989).  
[20] J. L. Tallon and J. W. Loram, Physica **C 349**, 53 (2001).  
[21] J. L. Tallon, J. W. Loram, J. R. Cooper, C. Panagopoulos, and C. Bernhard, Phys. Rev. **B 68**, 180501(R) (2003).  
[22] V. J. Emery and S. A. Kivelson, Nature (London) **374**, 434 (1995).  
[23] J. L. Tallon, C. Bernhard, H. Shaked, R. L. Hitterman, and J. D. Jorgensen, Phys. Rev. **B 51**, 12911 (1995).  
[24] V. M. Krasnov, Phys. Rev. **B 65**, 140504(R) (2002).  
[25] The different doping dependences of antiferromagnetic and superconducting (pairing) order implied by the SU(4) symmetry have been discussed in detail in Ref. [9], Section VII. There we show that the SU(4) symmetry requires that SC correlation energy decrease slower than the AF correlation energy as hole doping increases, implying that pairing inevitably wins with sufficient hole doping. The gap equations introduced in this paper represent a quantitative description of this competition.